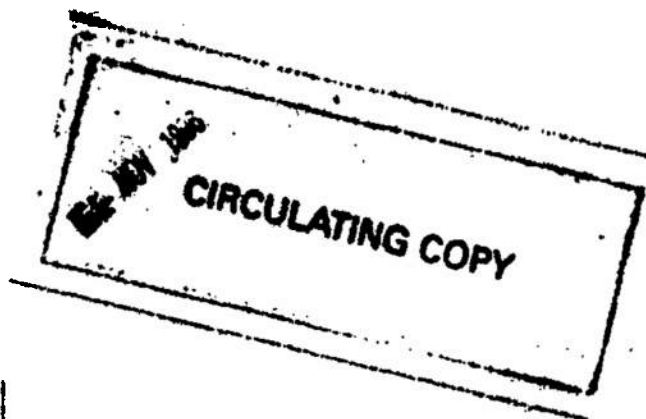


AD 250 146
PB 163 835

BRL



REPORT NO. 1118
OCTOBER 1960

FORECASTING THE FOCUS OF AIR BLASTS
DUE TO METEOROLOGICAL CONDITIONS
IN THE LOWER ATMOSPHERE

Beauregard Perkins, Jr.
Paul H. Lorrain
William H. Townsend

TECHNICAL LIBRARY
ANPR-LB (Slide 305)
ABERDEEN PROVING GROUND, MD. 21005

Department of the Army Project No. 5B03-04-002
Ordnance Management Structure Code No. 5010.11.815
BALLISTIC RESEARCH LABORATORIES



ABERDEEN PROVING GROUND, MARYLAND

und. 33895

BALLISTIC RESEARCH LABORATORIES

REPORT NO. 1118

OCTOBER 1960

FORECASTING THE FOCUS OF AIR BLASTS DUE TO
METEOROLOGICAL CONDITIONS IN THE LOWER ATMOSPHERE

Beauregard Perkins, Jr.

Paul H. Lorrain

William H. Townsend

Terminal Ballistics Laboratory

TECHNICAL LIBRARY

AMXBR-LB (Bldg. 305)

ABERDEEN PROVING GROUND, MD. 21005

Department of the Army Project No. 5B03-04-002

Ordnance Management Structure Code No. 5010.11.815

((Ordnance Research and Development Project No. TB3-0112))

ABERDEEN PROVING GROUND, MARYLAND

TABLE OF CONTENTS

	Page
ABSTRACT	3
ACKNOWLEDGEMENTS	5
LIST OF FIGURES.	6
BACKGROUND	7
BASIC THEORY	9
BLAST WAVE INTENSITY	23
DAMAGE CAUSED BY BLAST WAVES	26
GATHERING METEOROLOGICAL DATA.	26
FORECASTING THE FOCUS.	28
COMMENTS AND RECOMMENDATIONS	31
RECAPITULATION	32
REFERENCES	34
APPENDIX A	35
APPENDIX B	39

ERRATA Sheet for BRL Report No. 1018

Page 27. Figure 10 - Sample Data Sheet

Top two numbers in Columns 3, 4 and 5 should read:

3	4	5
Wind Direction From True North (Degrees)	Angle With Azimuth (Degrees)	Cos γ
300	94	-.07
012	166	-.97

BALLISTIC RESEARCH LABORATORIES

REPORT NO. 1118

BPerkins, Jr./PHLorrain/
WHTownsend/rac
Aberdeen Proving Ground, Md.
October 1960

FORECASTING THE FOCUS OF AIR BLASTS DUE TO
METEOROLOGICAL CONDITIONS IN THE LOWER ATMOSPHERE

ABSTRACT

Whenever explosions are used in testing or in experimental procedures, the sound waves that go beyond the limits of the installation may cause complaints of annoyance or damage from otherwise good neighbors. This is due to focusing of the sound waves caused by the meteorological conditions at the time of the explosion.

The theory of the propagation of sound through the atmosphere is given briefly. The conditions in the atmosphere which cause the sound to be focused are velocity gradients produced by variations with altitude of humidity, air temperature, and wind velocity. A simple method is described for evaluating these factors and forecasting the location of a focus, if one is to be expected, as well as the intensity of the sound at the focus.

This technique has been employed successfully at Aberdeen Proving Ground for three years during which time the complaints have been greatly reduced.

Intentionally Left Blank.

ACKNOWLEDGEMENTS

During the early stages of the investigation on which the procedures described in this report were based, the development of the Sperry-Rand "Electronic Ray Tracer" (Analogue Computer) became known to the authors. Through the courtesy of the Office of Naval Research and the Woods Hole Oceanographic Institution, the use of the Computer was made available for computing the ray paths. The work of Robert A. Lufburrow, of Woods Hole, who provided the ray paths for the first set of typical gradients, greatly accelerated the establishment of what is now our "Standing Operating Procedure".

Many of the early ray paths have been replaced by computed paths based on different gradients. These were provided by Willis Jackson and John Dorr using a later model computer. The many helpful suggestions of R. Shear concerning the presentation of the theory were greatly appreciated.

LIST OF FIGURES

	Page
Figure 1 - Plot of Equation 14 for Various Values of C_1 , i.e., for Different Angles of Departure θ	13
Figure 2 - Total Change in Velocity vs Altitude	14
Figure 3 - Ray Paths Corresponding to Gradients Represented In Figure 2.	15
Figure 4 - Range and Altitude for a Given Ray in a Medium Of a Single Gradient	16
Figure 5 - Range of Ray in a Medium of Two Layers Having Velocity Gradients of K_1 and K_2	18
Figure 6 - Diagram Defining Terms in Equation 21.	21
Figure 7 - Plot of Travel Time and Range vs Angle Of Departure	22
Figure 8 - Surface Air Blast Pressure vs Range From Detonation of Various Weights of High Explosives Fired on the Surface	24
Figure 9 - Various Types of Velocity Gradients to be Expected and the Increase in Intensity at a Focus for Each Type.	25
Figure 10 - Sample Data Sheet.	27
Figure 11 - Plot of Total Change in Velocity vs Altitude	29
Figure 12 - Ray Paths Corresponding to Gradients Represented In Figure 11	30

BACKGROUND

At every Department of Defense establishment where testing operations involve the explosion of H.E. charges outdoors, there are frequent complaints of annoyance or claims for damage from persons living in contiguous areas. The complaints of annoyance are often justified; the damage claims are often unjustified. Both can be reduced or avoided entirely.

The refraction of sound waves produced by the meteorological conditions between the earth's surface and the elevation of 10,000 to 12,000 feet may cause the sound waves produced by explosions at or above the surface of the ground to be focused near homes in the vicinity of the testing area. This phenomenon may be annoying; however, it is doubtful that any damage to walls or window glass will be caused by air blast at distances greater than a few miles from any but very large explosions (100 or more pounds of high explosive).

The refraction of the sound waves is due to the presence of vertical gradients of the velocity of sound through the air ($\frac{dv}{dy}$) where v is the velocity of sound and y is the altitude. Since the velocity of sound in air depends on temperature, humidity, and the wind, the vertical gradient will depend on variations of these factors with altitude.

One of the earliest papers on the refraction of sound due to meteorological conditions was presented to the Royal Society of London about 1906 as a result of the firing of guns during the funeral of Queen Victoria. The easily recognized noise resulting from the rhythmic firing of the guns was heard in London and also far to the north but the two areas were separated by a zone of silence. This experience was explained by refraction due to a wind, directed to the north, with a large wind gradient existing at high altitudes. Since that time, about sixty papers have been published on this subject. Everett F. Cox⁽¹⁾, in his treatment

(1) Numerals refer to references listed at end of the report.

of upper air temperatures as measured at the demolition of Helgoland, has reviewed the salient facts and presented an excellent bibliography of the important contributions.

In the present paper, nothing has been added to the classical theory of propagation; however, an operation procedure is described that permits the meteorological conditions to be quickly evaluated and the cause of complaints from contiguous areas reduced to a minimum.

BASIC THEORY

As stated previously, the velocity of sound in the atmosphere depends on temperature, humidity, and wind. Experience shows that the temperature of the lower atmosphere at Aberdeen Proving Ground may vary through a range of 20 to 30°C between the surface and an altitude of 10,000 feet, causing a change in velocity of sound of 40 to 60 feet per second. In this same region, the wind may vary from 0 to 45 or 60 feet per second. Although the change in relative humidity can be as large as 50%, such a change can affect the velocity of sound by only about 1 foot per second. Since 1 foot per second is less than the error in our determination of wind velocities, the effect of changes in humidity can be neglected without noticeable error.

When the problem of devising a simple but safe set of guidance rules for firing at Aberdeen Proving Ground was given to the Ballistic Research Laboratories, a study was made of the meteorological conditions prevailing in the vicinity of Aberdeen on those days when complaints had been registered. Of twenty-six cases, in all but one, there was a strong wind increasing in velocity at altitudes of about two or three thousand feet up to eight or ten thousand feet. The wind was in general from the point of detonation toward the point of complaint. This fact was taken as sufficient evidence that any guidance rules for the Aberdeen Proving Ground area should include consideration of wind effects in addition to the effect of temperature on the propagation of the sound waves. Thus velocity gradients are based on an algebraic sum of the temperature effect and the wind effect at each altitude. The temperature effect is of course a scalar quantity and is the same in all directions, whereas the wind effect is a vector quantity and is a function of direction. Before describing how the temperature and wind effects can be calculated, the nature of the paths of sound waves will be reviewed briefly.

When an explosion occurs at the surface of the ground, a diverging shock front starts at the point of explosion and spreads in all directions in the hemisphere above the surface of the ground. The shock waves degenerate to sound waves quite rapidly and it is sufficient for

the purpose of this study to consider only the propagation of sound waves.

The paths of the various parts of the wave front can be depicted by rays emanating in all directions from the center of the explosion. One of these rays will start from the source making an angle θ with the horizontal. Then at the surface

$$y' = \frac{dy}{dx} = \tan \theta$$

where x and y are the horizontal and vertical coordinates. If θ_y is the angle between the ray and the horizontal at any altitude y :

$$y' = \frac{dy}{dx} = \tan \theta_y \quad (1)$$

and
$$y'' = \frac{d^2 y}{dx^2} = \frac{d(\tan \theta_y)}{dx} \quad (2)$$

If the velocity of sound varies with altitude, the angle θ will vary according to Snell's law such that, if V_y is the velocity at altitude y , then

$$\frac{\cos \theta_y}{V_y} = \text{a constant} = C \quad (3)$$

or
$$\cos \theta_y = CV_y \quad (4)$$

from (1)
$$y' = \frac{\sin \theta_y}{\cos \theta_y} \quad (5)$$

from (4) and (5)
$$y' = \frac{\sqrt{1 - (CV_y)^2}}{CV_y} \quad (6)$$

or
$$y' = \sqrt{\left[\frac{1}{CV_y}\right]^2 - 1} \quad (7)$$

and

$$y'' = \frac{-1}{c^2 v_y^3} \frac{dv_y}{dy}$$

$$y'' = \frac{-1}{v_y \cos^2 \theta_y} \frac{dv_y}{dy} \quad (8)$$

$$= \frac{-1}{v_y} (\sec^2 \theta_y) \frac{dv_y}{dy} \quad (9)$$

$$= \frac{1}{v_y} \left[1 - (y')^2 \right] \frac{dv_y}{dy} \quad (10)$$

If $\frac{dv_y}{dy} = \text{a constant } K$ (the vertical velocity gradient) and if $V_1 = \text{velocity at the ground surface, then}$

$$v_y = V_1 + Ky \quad (11)$$

$$= K \left(\frac{V_1}{K} + y \right) \quad (12)$$

and

$$y'' = - \left[\frac{1}{K \left(\frac{V_1}{K} + y \right)} \right] \left[1 + (y')^2 \right] K$$

$$= - \left[\frac{1 + (y')^2}{\frac{V_1}{K} + y} \right] \quad (13)$$

The solution of equation 13 (see references 1, 2, and 3) represents the path of propagation with least time between two points:

$$(x + C_2)^2 + \left(y + \frac{V_1}{K}\right)^2 = C_1^2 \quad (14)$$

in which C_1 and C_2 are constants of integration, and x and y are the cartesian coordinates of the points along the ray path. Equation 14 represents a circle the center of which is on a line below the ground surface a distance equal to V_1/K . The parameter C_1 is the radius of

the circle and C_2 is the horizontal distance from the origin of coordinates to the center of the circle. In Figure 1 are shown the paths of several rays starting at the source with different angles of departure. For a negative gradient the path of the sound wave would be the arc of a circle curving upward, the center of the circle being on a line above the ground surface at a distance equal to V_1/K .

Variations with altitude of either the rate of change in air temperature or the rate of change in wind velocity will change the value of the gradient K and therefore the curvature and direction of the corresponding arc will change accordingly. At the boundary between layers having different values of K there will be a layer of transition in which the conditions gradually change from those of one layer to those of the other. In this transition layer the path of a ray gradually changes from the arc determined by the velocity gradient in the layer from which the ray is emerging to the arc determined by the gradient of the layer being entered. Figure 2 shows a typical graph of sound velocity versus altitude and Figure 3 shows the paths of the rays resulting from the gradients in Figure 2. As indicated above, the curvature of the paths in any layer depends on the gradient in the layer.

For a ray to be refracted to the surface from any layer, the maximum velocity attained in that layer must equal or exceed the velocity at all points in the medium nearer the surface of the ground.

If the ray path is confined to a medium in which only a single velocity gradient exists the horizontal distance traversed by a given ray (i.e. the range) can be most simply calculated by plane geometry. In Figure 4 a ray path is shown leaving the origin at an angle θ , rising in an arc to an altitude y and returning to the surface at a horizontal distance R from the origin.

In the figure,

$$\tan \theta = \frac{R/2}{V_1/K}$$

or

$$R = 2 (V_1/K) \tan \theta$$

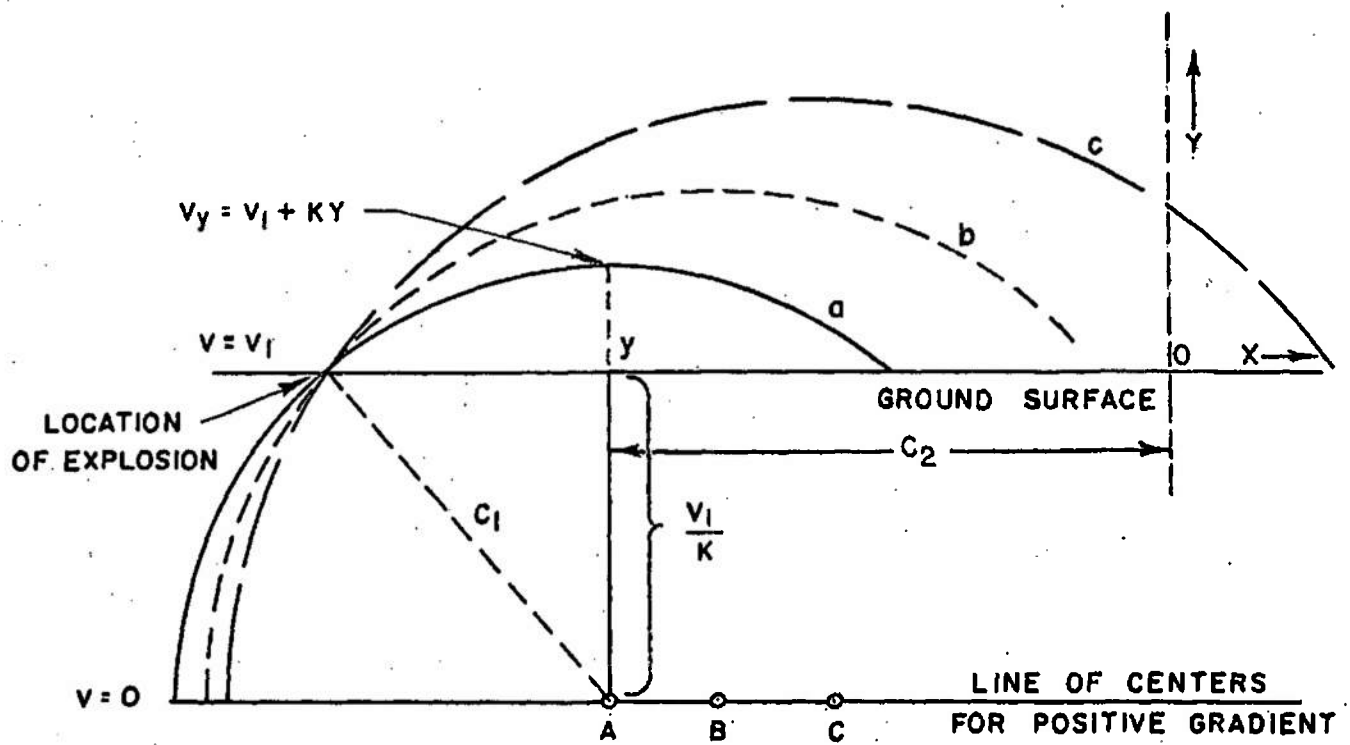


FIG. 1 - PLOT OF EQUATION 14 FOR VARIOUS VALUES OF C_1 ,
i.e. FOR DIFFERENT ANGLES OF DEPARTURE

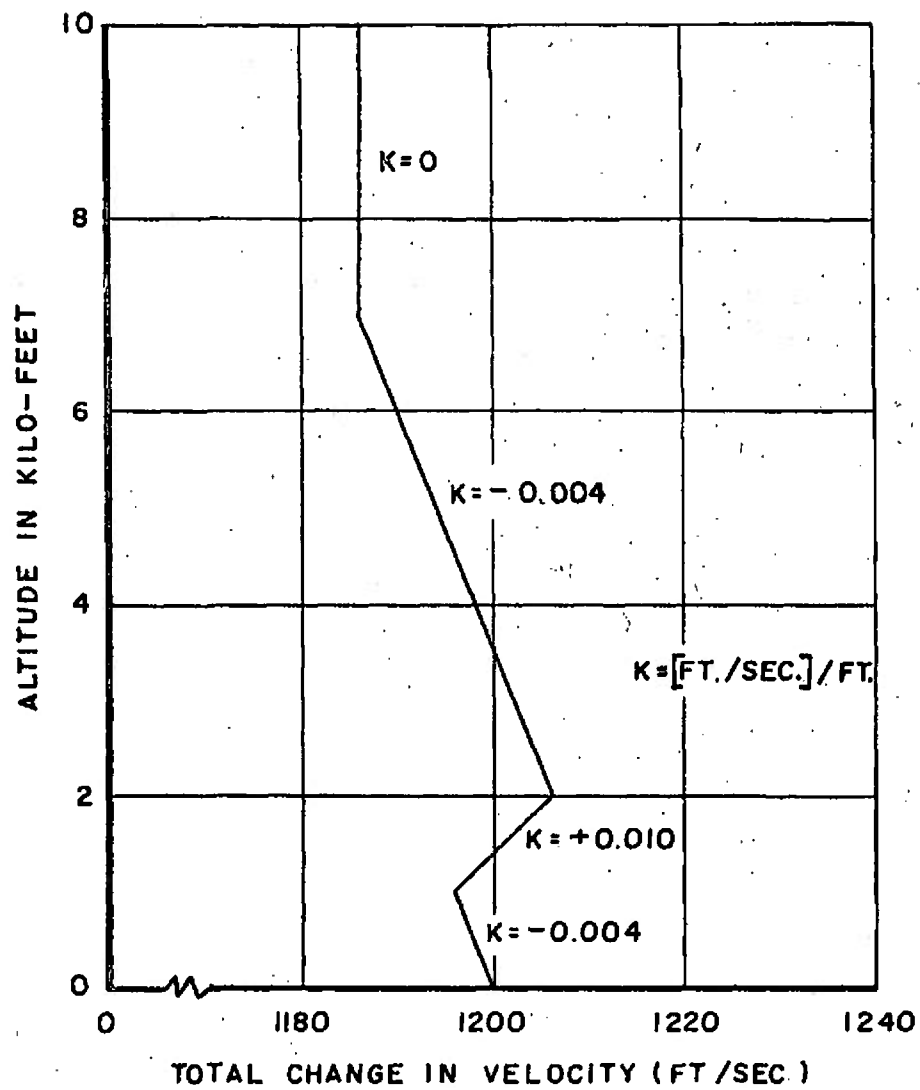


FIG 2-TOTAL CHANGE IN VELOCITY vs. ALTITUDE

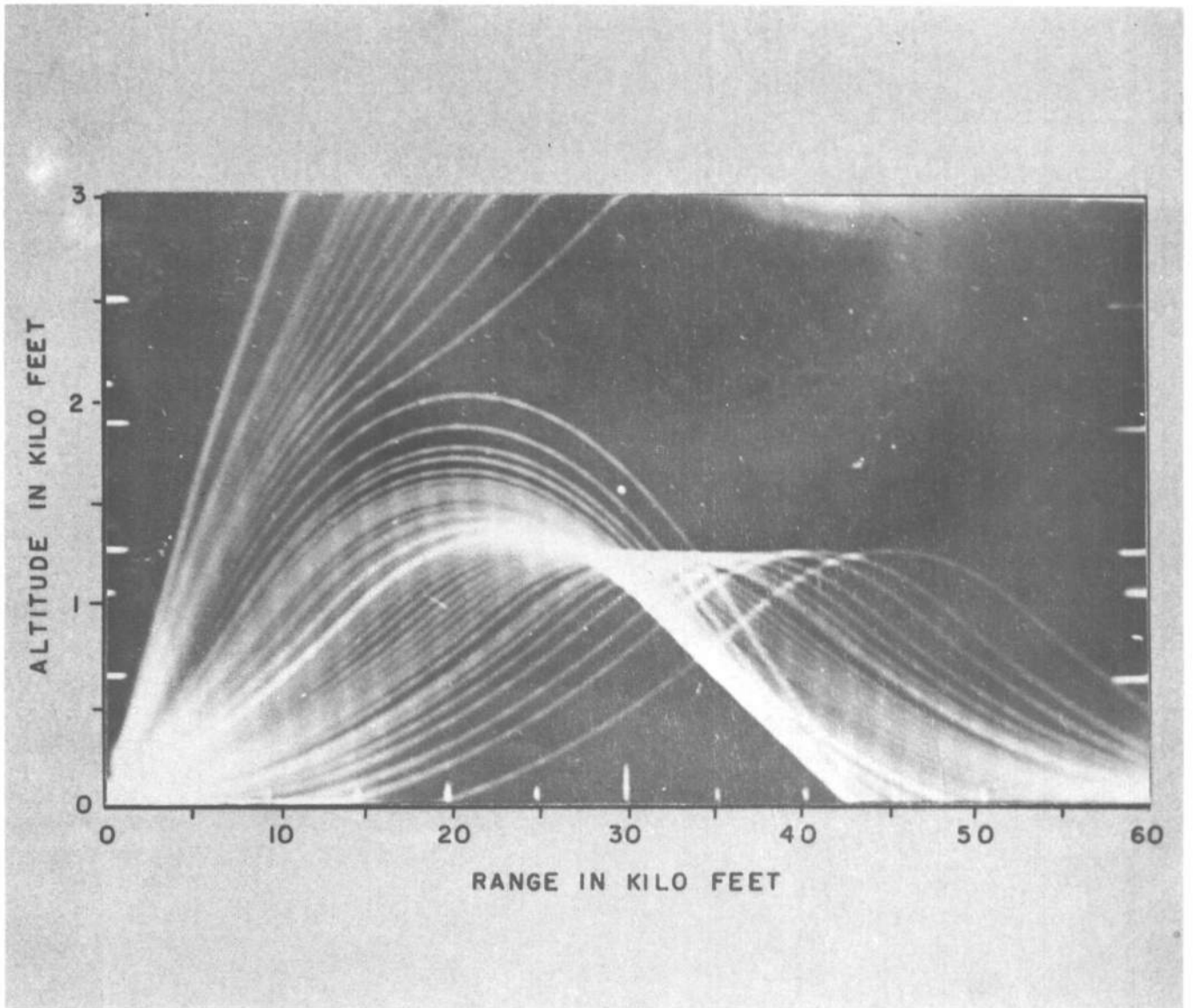
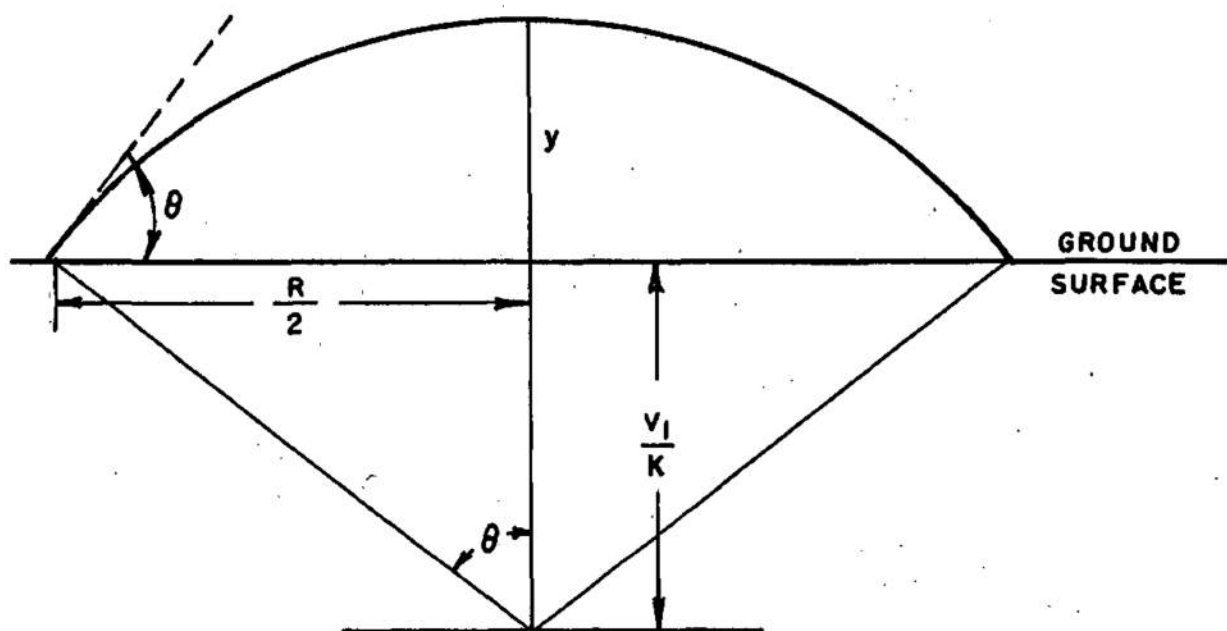


FIG. 3-RAY PATHS CORRESPONDING TO GRADIENTS
REPRESENTED IN FIG. 2



θ = ANGLE OF DEPARTURE
 R = HORIZONTAL RANGE
 y = MAXIMUM ALTITUDE REACHED BY THE RAY.

FIGURE 4.- RANGE AND ALTITUDE FOR A GIVEN RAY IN A MEDIUM OF A SINGLE GRADIENT

where V_1 = initial velocity and K is the velocity gradient.

The travel time $t = 2 \int_0^y \frac{ds}{V_y}$

in which $ds = \left[(dx)^2 + (dy)^2 \right]^{1/2}$

and $V_y = V_1 + Ky$

After integration:

$$t = \frac{2}{K} \log \cot \left(\frac{\pi}{4} - \frac{\theta}{2} \right)$$

For a medium having two gradients the path of a ray is pictured in Figure 5. The range of the ray departing at an angle θ_1 will be:

$$R = 2X_1 + 2X_2$$

$$X_1 = ac - bc$$

$$ac = \frac{V_1}{K_1} \tan \theta_1$$

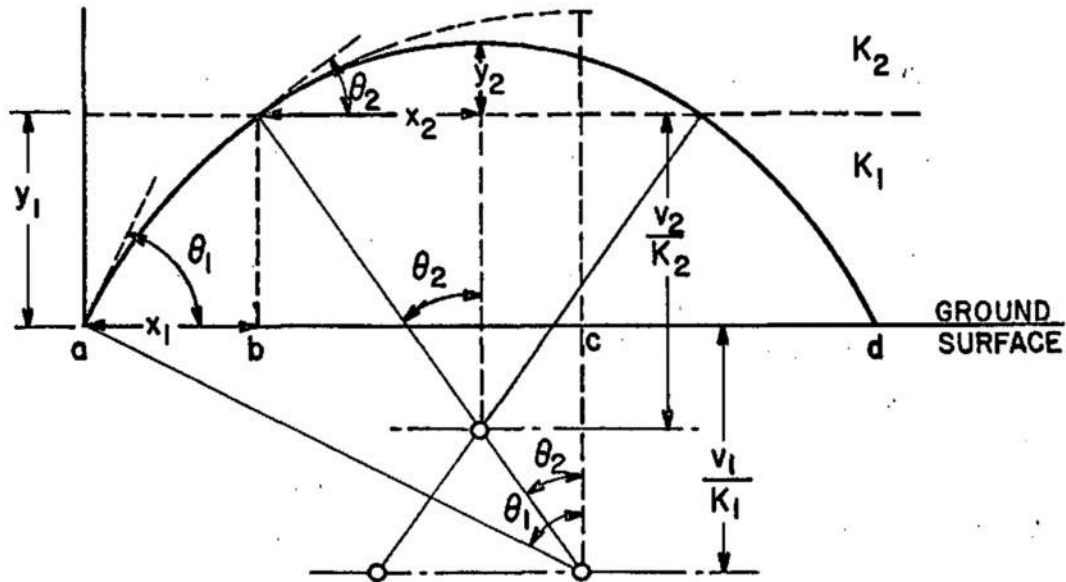
$$bc = \left(\frac{V_1}{K_1} + y_1 \right) \tan \theta_2$$

Since $V_2 - V_1 = K_1 Y_1$ then $y_1 = \frac{V_2}{K_1} - \frac{V_1}{K_1}$

and $X_1 = \frac{V_1}{K_1} \tan \theta_1 - \frac{V_2}{K_1} \tan \theta_2$

$$X_2 = \frac{V_2}{K_2} \tan \theta_2$$

and $R = \frac{2V_2}{K_2} \tan \theta_2 + \frac{2V_1}{K_1} \frac{\sin \theta_1}{\cos \theta_1} - \frac{2V_2}{K_1} \frac{\sin \theta_2}{\cos \theta_2}$



θ_1 = ANGLE BETWEEN RAY AND HORIZONTAL AT SURFACE.
 θ_2 = ANGLE BETWEEN RAY AND HORIZONTAL AT TOP OF LAYER.
 $a d$ = RANGE OF RAY = $2x_1 + 2x_2$.
 K_1, K_2 = GRADIENTS IN 1st AND 2nd LAYER RESPECTIVELY.

FIGURE 5 - RANGE OF RAY IN A MEDIUM OF TWO LAYERS
 HAVING VELOCITY GRADIENTS OF K_1 & K_2

which reduces to:

$$R = \frac{2V_2}{K_2} \tan \theta_2 + \frac{2V_1}{K_1 \cos \theta_1} (\sin \theta_1 - \sin \theta_2) \quad (20)$$

The travel time for the two layered medium is

$$t = 2 \int_0^{y_1} \frac{ds}{V_y} \quad (\text{for 1st layer}) + 2 \int_{y_1}^{y_2} \frac{ds}{V_y} \quad (\text{for 2nd layer})$$

For 1st layer

$$t_1 = 2 \int_0^{y_1} \frac{ds}{V_y} \text{ in which } ds = \left[(dx)^2 + (dy)^2 \right]^{1/2} \text{ and } V_y = V_1 + Ky$$

$$t_1 = 2 \int_0^{y_1} \frac{\left(\frac{1}{\sin \theta} \right) dy}{V_1 + Ky} = 2 \int_{\theta_1}^{\theta_2} \frac{-d\theta}{K_1 \cos \theta}$$

$$= - \frac{2}{K_1} \log \tan \left(\frac{\pi}{4} + \frac{\theta}{2} \right) \Bigg|_{\theta_1}^{\theta_2}$$

$$= \frac{2}{K_1} \left[\log \tan \left(\frac{\pi}{4} + \frac{\theta_1}{2} \right) - \log \tan \left(\frac{\pi}{4} + \frac{\theta_2}{2} \right) \right]$$

$$= \frac{2}{K_1} \left[\log \cot \left(\frac{\pi}{4} - \frac{\theta_1}{2} \right) - \log \cot \left(\frac{\pi}{4} - \frac{\theta_2}{2} \right) \right]$$

For 2nd layer

$$t_2 = 2 \int_{y_1}^{y_2} \frac{ds}{V_y} \text{ in which } V_y = V_2 + K_2 y$$

$$= \frac{2}{K_2} \log \cot \left(\frac{\pi}{4} - \frac{\theta_2}{2} \right)$$

The total travel time $t = t_1 + t_2$

$$t = \frac{2}{K_1} \left[\log \cot \left(\frac{\pi}{4} - \frac{\theta_1}{2} \right) - \log \cot \left(\frac{\pi}{4} - \frac{\theta_2}{2} \right) \right] + \frac{2}{K_2} \log \cot \left(\frac{\pi}{4} - \frac{\theta_2}{2} \right) \quad (21)$$

The symbols of equation (21) are defined in the diagram of Figure 6.

Figure 7 presents a plot of the travel time (t) versus angle of departure (θ) and range (R) versus θ for the case of transmission through an atmosphere in which two velocity gradients K_1 and K_2 exist, K_1 being less than K_2 . It should be noted that at $\theta = \theta_1$ the travel time curve and the range pass thru a minimum. Furthermore, both the travel time and range change very slowly with θ in the vicinity of θ_1 . This indicates that for the conditions stated for Figure 7, a cone of rays will be converged at a range of R_1 with very slight differences in phase which will produce an increase in intensity. The various combinations of gradients that will produce this focussing is of vital interest and can best be shown by calculating ray paths for various combinations of gradients that can be expected to occur. An analogue computer has been used to calculate and trace ray paths for single gradients and for combinations of two to seven gradients. The solutions show paths for a group of rays starting at different angles of departure. If focussing occurs the convergence will be shown as well as the distance to the point of focus.

The Piedmont Division of Sperry-Rand Corporation, Charlottesville, Virginia, designed the analogue computer used. With it the effect of from one to twenty gradients can be considered. The computer is small in volume (about two cubic feet) and provides the solution in a few minutes. In order to simplify the construction of the computer some simplifying assumptions were made in the solution of the equation of the ray path. The approximations and the resulting errors are insignificant. This is demonstrated in Appendix A.

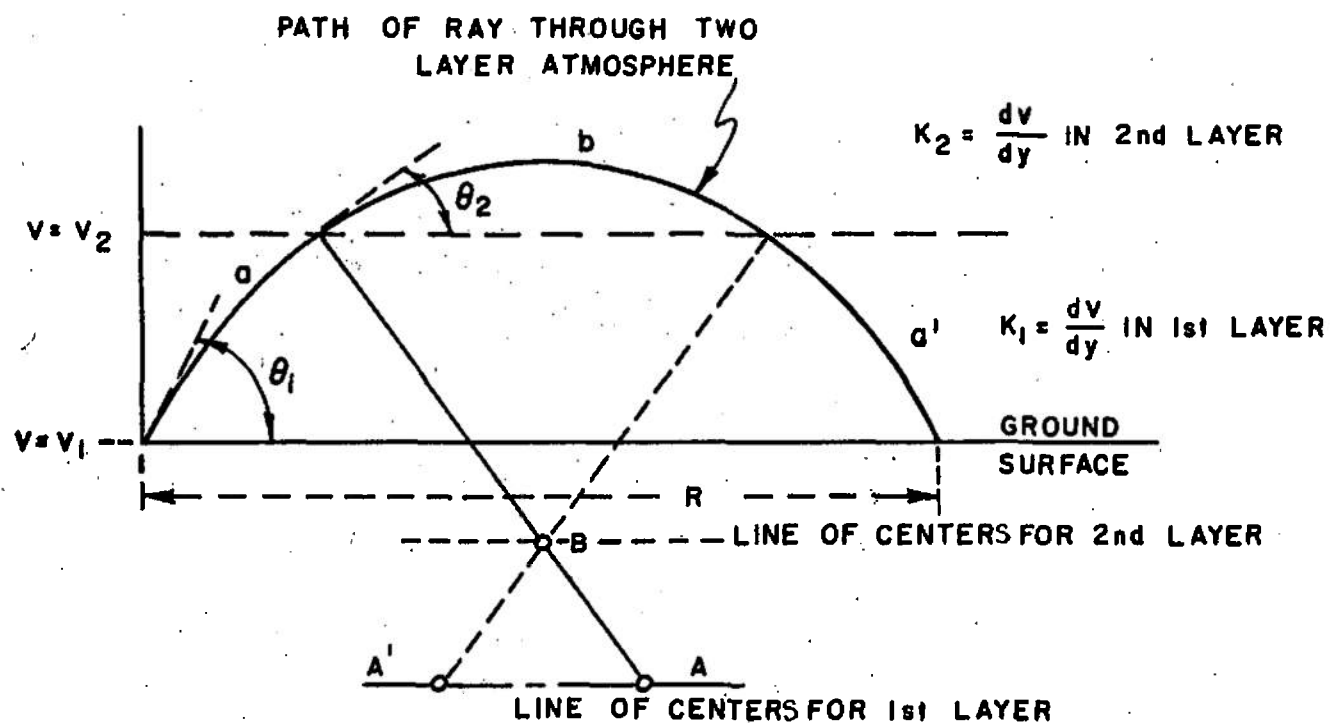


FIG 6-DIAGRAM DEFINING TERMS IN EQUATION 21

TECHNICAL LIBRARY
ANXER-LB (Blde. 305)
ABERDEEN PROVING GROUND, MD. 21095

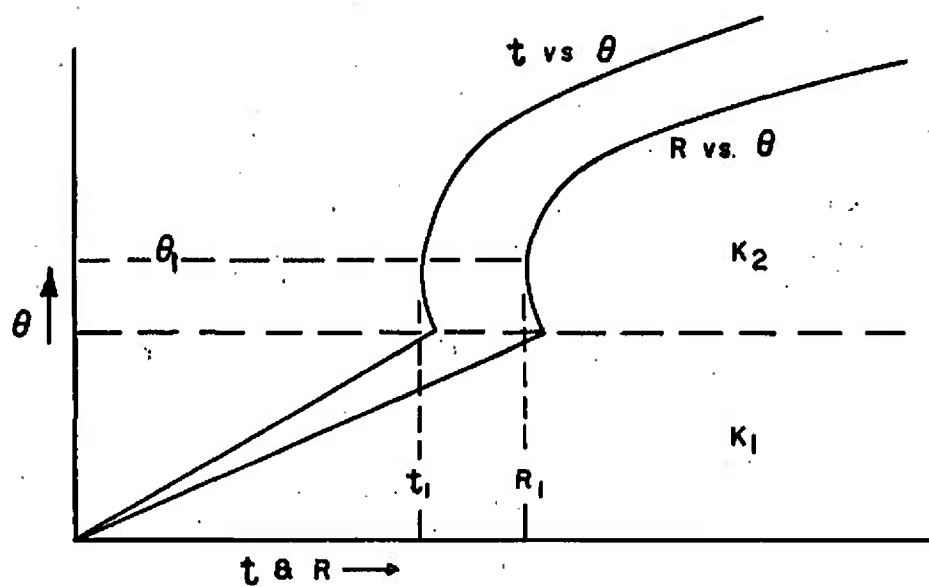


FIG. 7 - PLOT OF TRAVEL TIME AND RANGE vs. ANGLE OF DEPARTURE θ

BLAST WAVE INTENSITY

The overpressure in a blast wave when propagated through an atmosphere in which the velocity gradient is zero has been determined for various distances for several different weights of explosive. At a given distance the overpressure in the blast wave will be different if the explosive is detonated at the surface of the ground or in free air. The measured value will also be different if the pressure gage is at the surface of the ground or in free air. In Figure 8 graphs are shown which give the overpressure versus distance for several weights of explosive detonated at the surface and the overpressure measured at the surface for a uniform atmosphere.

When the ray paths of sound are affected by gradients in the atmosphere the intensity at a given distance will be some multiple of the overpressure given in Figure 8 for the given distance. The combinations of gradients to be experienced can be classed as one of five basic types or categories. The types are shown in Figure 9. For each type approximate values have been determined for a "multiplication factor" to calculate the intensity at a focus due to that type of gradient combination.

The value of intensity at a focus compared to the intensity at the same distance in a uniform atmosphere has been derived from the experience of several years. A few direct and many indirect determinations have been made. By noting the distance to a particular type of damage and assuming the minimum overpressure known to produce such damage, a maximum "multiplication factor" can be calculated. Such indirect methods have provided conservative but very useful values for calculating overpressures to be expected. The calculation of the intensity to be expected at the focus is made as follows:

The distance from the explosion to the focus is noted in the solution on the computer, and the intensity of the blast wave at that distance in a uniform atmosphere is read from Figure 8. The category of the gradient combinations in the atmosphere is determined by comparison of the velocity versus altitude curve with Figure 9 and the

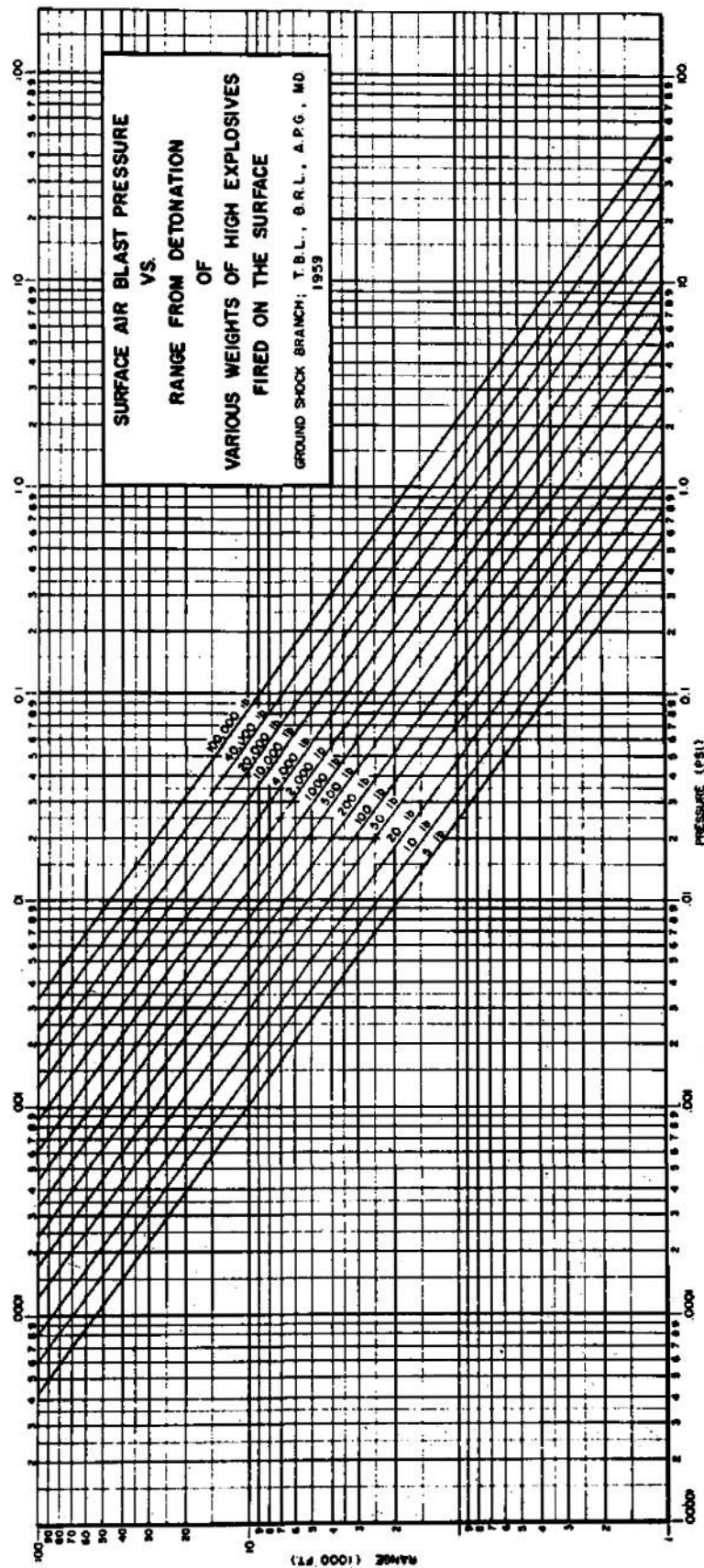


FIG. 8

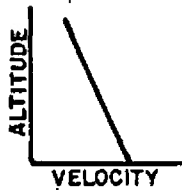
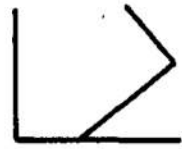
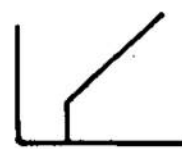
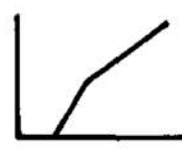

CATEGORY	DESCRIPTION		MULTIPLICATION FACTOR
1	SINGLE NEGATIVE GRADIENT		0
2	SINGLE POSITIVE GRADIENT		5
3	ZERO GRADIENT NEAR SURFACE WITH POSITIVE GRADIENT ABOVE		10
4	WEAK POSITIVE GRADIENT NEAR SURFACE WITH STRONG POSITIVE GRADIENT ABOVE		25
5	NEGATIVE GRADIENT NEAR SURFACE WITH STRONG POSITIVE GRADIENT ABOVE		100

FIG. 9 - VARIOUS TYPES OF VELOCITY GRADIENTS TO BE EXPECTED AND THE INCREASE IN INTENSITY AT A FOCUS FOR EACH TYPE.

"multiplication factor" is observed. The intensity read from Figure 8 multiplied by the "multiplication factor" will be the intensity at the focus to be expected.

DAMAGE CAUSED BY BLAST WAVES

The damage caused by the overpressure of a blast wave depends to a very large extent on the type of construction. Glass panes of average size and thickness vary greatly in their ability to withstand blasts depending on how the panes are mounted. If the pane is forced into the frame so as to be under a constant strain, a blast wave of 0.1 psi overpressure can cause the pane to crack but if it is mounted without any strain in the glass an overpressure of about 0.75 psi may be required to crack it.

The cracking of plaster on a wall depends on the flexibility of the wall. A plastered surface attached to a masonry wall will withstand a much higher pressure than a surface supported by a wide wooden panel. In general a well constructed plastered wall will stand higher overpressures than average window panes.

An overpressure of .03 to .05 psi in a blast wave can cause a loose window sash to slap the window frame and produce a loud noise while actually no damage is being done. In contrast to this, the quiet settling of one corner of a house can cause damage to walls and windows which is often attributed to blast waves.

GATHERING METEOROLOGICAL DATA

The meteorological data are gathered by release of a weather balloon and radiosonde. A GMD 1 A Rawin set is used at Aberdeen Proving Ground. The wind data are calculated from the successive positions of the balloon which is determined at frequent intervals. The air temperature is telemetered back by the radiosonde. From the ground surface to 5000 feet altitude, the temperature and wind velocity and direction should be determined for 500 feet intervals. From 5000 feet to about 12000 feet the data should be determined every 1000 feet. The data are recorded as in the sample data sheet (Figure 10). The air temperature is recorded in degrees centigrade. A change in temperature

METEOROLOGICAL DATA

APG

RELEASE TIME 1243 HRS. DATE 13 NOV. 1959

AZIMUTH OF INTEREST 206°

1	2	3	4	5	6 7		8	9	10
AIR TEMP. °C	ALTITUDE ABOVE SURFACE (FEET)	WIND DIRECTION FROM TRUE NORTH (DEGREES)	ANGLE WITH AZIMUTH γ° (DEGREES)	COS γ	WIND VELOCITY		COMP OF WIND FT/SEC	ΔV DUE TO TEMP FT/SEC	TOTAL CHANGE VELOCITY FT/SEC
					MI/HR	FT/SEC			
15.1	0	030	86	.07	5	7.3	-1	30	29
12.0	720	102	14	.97	7	11	-10	24	14
11.5	1200	162	44	.72	11	16	11	23	34
11.0	1790	193	13	.97	14	21	20	22	42
9.5	2320	201	5	.99	14	21	20	19	39
9.5	2910	194	12	.98	17	25	24	19	43
8.2	3440	201	4	.99	19	28	28	16	44
6.9	4520	216	10	.98	22	32	32	14	46
5.2	5600	216	10	.98	23	34	33	10	43
3.0	6680	210	4	.99	25	37	36	6	42
1.3	7820	208	2	.99	24	35	35	3	38
0.9	8850	220	14	.97	22	32	31	2	33
0.2	9700	231	25	.90	27	40	36	0	36
-1.4	10750	235	29	.87	30	44	39	-3	36

NOTE:

IN COLUMN 3 - RECORD DIRECTION TO WHICH WIND IS BLOWING

IN COLUMN 4 - ANGLE BETWEEN WIND DIRECTION AND AZIMUTH OF INTEREST

IN COLUMN 8 - (WIND VELOCITY AT EACH ALTITUDE) x (COS γ AT SAME ALTITUDE)

IN COLUMN 9 - (VALUE IN COLUMN 1 AT EACH ALTITUDE) x 2.

COLUMN 10 IS THE SUM OF COLUMNS 8 AND 9

FIGURE 10—SAMPLE DATA SHEET

of the air of 1°C changes the velocity of sound almost exactly 2 feet/second, so the difference between the velocity of sound at a given temperature and the velocity at 0°C is determined by multiplying the temperature by 2. Since the effect of wind varies with direction, the component of the wind in the direction of interest must be calculated for each elevation.

At each elevation, the sum of the component of the wind in the direction of interest (column 8 in Figure 10) and the change in velocity due to the temperature (column 9) will give the difference between the velocity at that elevation and the velocity at zero degrees centigrade. If the values of this resultant (column 10) are plotted on linear coordinates as in Figure 11, the variation in velocity is depicted and the magnitude of the gradients can be measured. Figure 11, is the presentation of the data upon which the forecast of a focus and its location is based. If the wind varies widely in direction with altitude, it may be necessary to reduce the data for two or more directions, each case being treated separately as described above.

FORECASTING THE FOCUS

If the velocity data shown in Figure 11 are furnished to the Sperry-Rand analogue computer, a presentation of the resulting ray paths will be shown on the screen. Ray paths corresponding to the conditions depicted in Figure 11 are shown in Figure 12. If a focus occurs, it will be seen on the screen where the rays converge and the distance from the source will be shown.

Actually at APG, it has been found that the pattern of gradients often repeat so that a library of 32 "typical gradients" and the resulting ray paths have been accumulated. Generally the gradients recorded daily can be matched sufficiently close with one of the "typical gradients" to be used for a forecast. The computer should be kept at hand for more precise determination when needed and for those cases for which there is no matching typical gradient. The typical gradients are included in Appendix B.

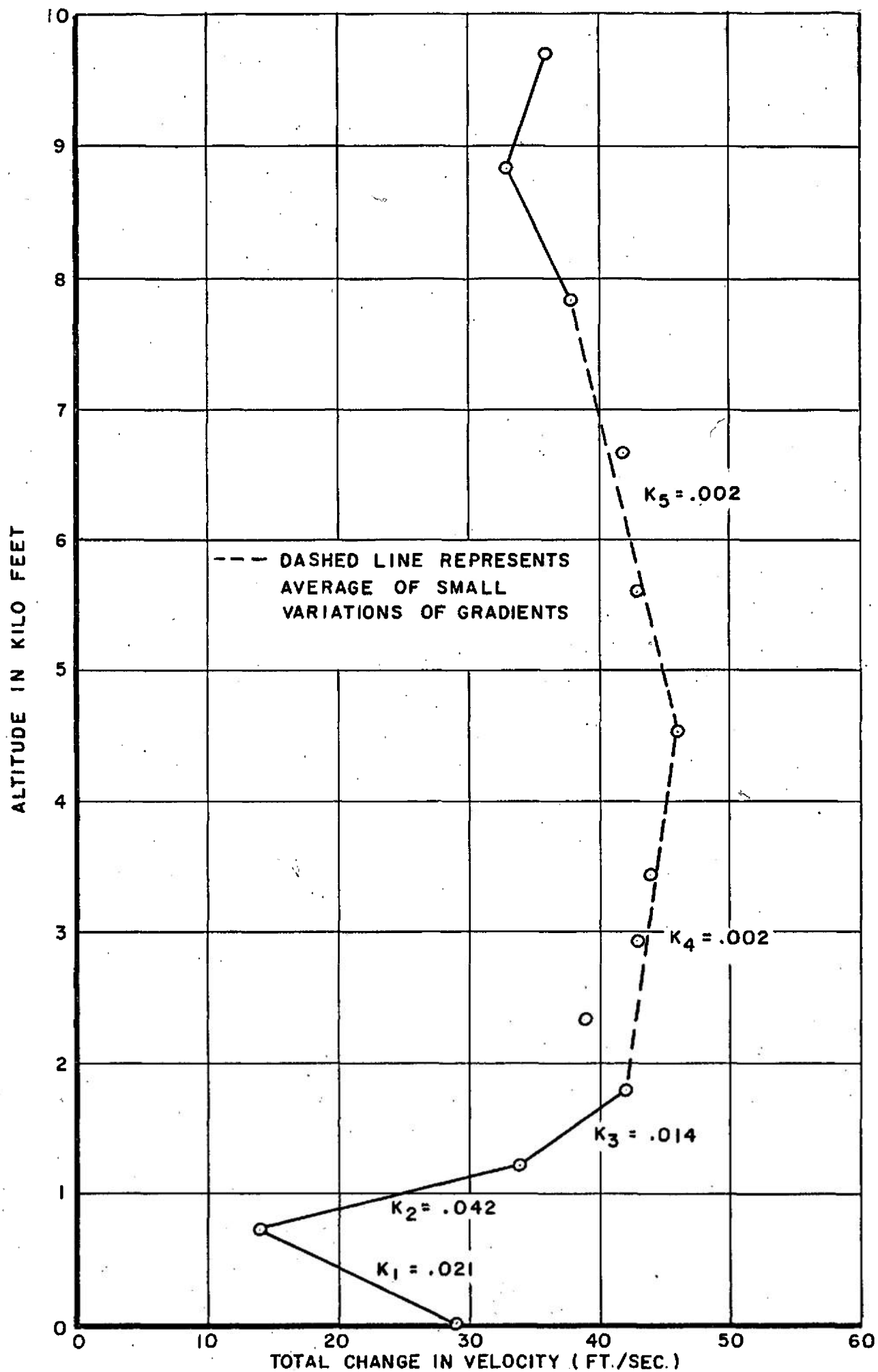


FIG II-PLOT OF TOTAL CHANGE IN VELOCITY vs. ALTITUDE

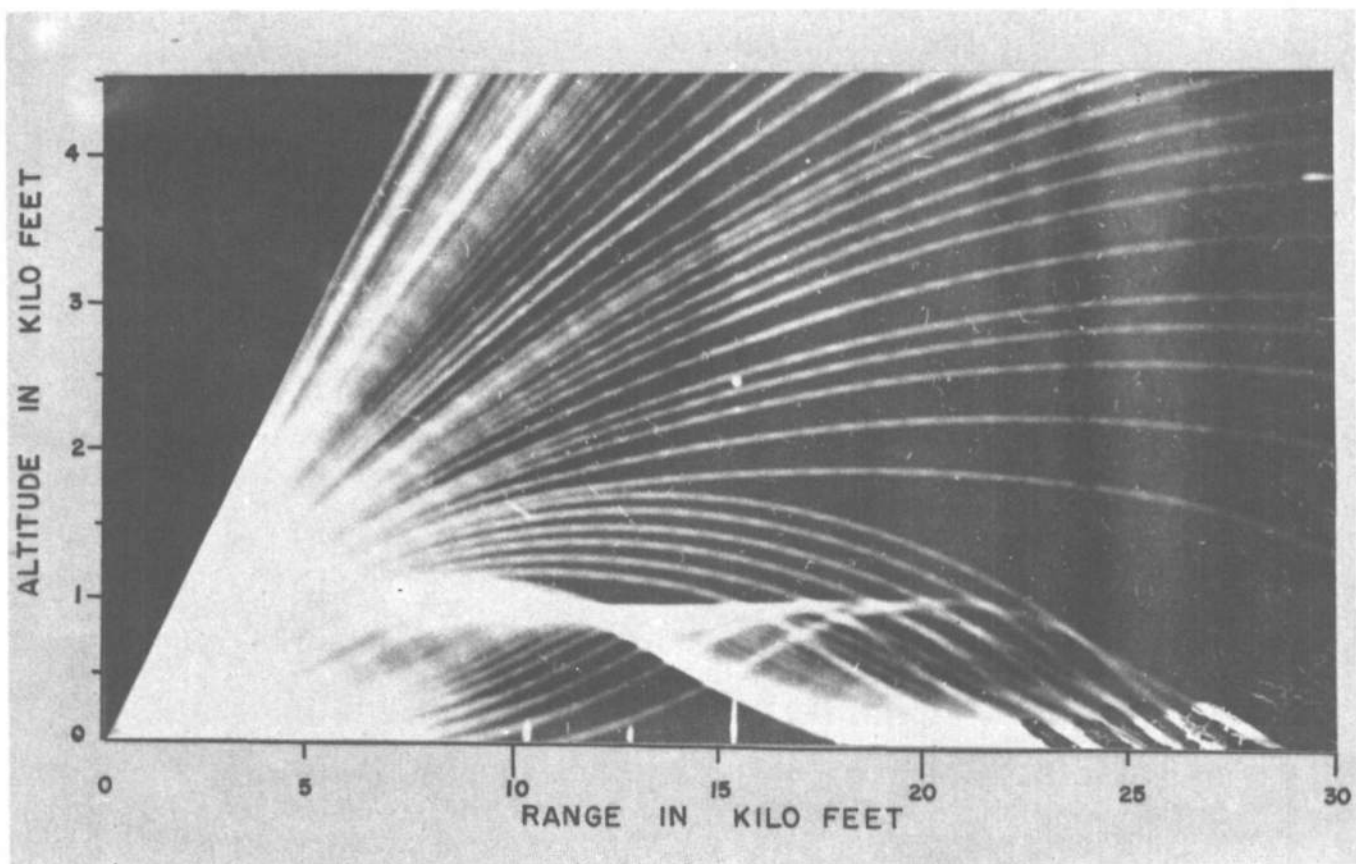


FIG.12 - RAY PATHS CORRESPONDING TO GRADIENTS
REPRESENTED IN FIG. II

COMMENTS AND RECOMMENDATIONS

When a government establishment is put in an isolated area, the regions just beyond the exits may soon be occupied by non-government employees desiring to supply goods or services and the area may become a site for housing developments.

If possible, a test center involving the use of explosives should be so located that the prevailing upper winds will blow from the source of blast waves toward a wide stretch of Government owned lands or to the open sea.

The entrances to the establishment should be so located that the prevailing upper winds will blow from them toward the point of detonation.

The direction of the winds are determined by the position of the high and low pressure areas in the atmosphere and with a little experience in this procedure a study of the daily weather maps will permit a meteorologist to forecast good shooting periods several days in advance. Since the conditions in the atmosphere usually drift toward the east, the preceding statement will be of no help to stations along the Pacific Coast because no detailed data for the area immediately west of the coast is given on the weather maps.

The most desirable time for detonating an explosive is when the center of a high pressure area is at the point of detonation. The temperature of the air around the test site will then be found to decrease with altitude and the wind will be at a minimum. Under such conditions, the blast waves are refracted upward and the detonation of a large charge (1000 pounds of TNT) would be barely audible at a distance of one or two miles.

Generally the weather conditions change slowly, since the areas of high and low atmospheric pressures are large and on the average move only 300 miles per day. Therefore the conditions indicated by the meteorological data can be expected to remain sufficiently constant for about 8 hours. The firing should be started as soon as possible after the meteorological data are taken. If the firing is to extend from daylight

conditions into the night, it is advisable to make a "metro" run in the late afternoon to detect any changes that are occurring. If the weather map shows a "weather front" to be approaching caution in the firing is advisable. Firing should be discontinued during the passing of the "front" and a metro run should be made after the passage of the "front" to determine if firing can be resumed.

It should be noted that the worst focusing conditions can cause the pressures indicated in Figure 8 to be multiplied by 100. If the weight of the explosive being detonated is so small that the pressure at the nearest point of possible damage could not exceed 0.1 psi even under the worst conditions, then firing can proceed without a metro run. This procedure will sometimes cause complaints of annoyance but should not result in damage.

RECAPITULATION

The following summary of the Standard Operating Procedure will serve as a convenient guide:

1. The meteorological balloon should be released 2 or 3 hours before the firing program is scheduled to begin.
2. The wind and temperature data should be reduced and tabulated as in Figure 10. Data should be recorded at intervals of 500 feet from the surface to 5000 feet altitude and at intervals of 1000 feet from 5000 feet to 12000 feet altitude.
3. The velocity versus altitude should be plotted for each azimuth of interest as in Figure 9 and the velocity gradients should be noted.
4. The combination of gradients for each azimuth should be compared to the set of 32 in Appendix B and the location of the focus (if one is indicated) should be noted.

(If no sample velocity versus altitude curve in Appendix B can be found to match the one just plotted then the analogue computer must be used.)

5. With the weight of explosives to be detonated and the distance to the focus known, the pressure to be expected in a uniform atmosphere

can be read from the chart on Figure 8 of the text.

6. By comparing the velocity versus altitude curve to the five basic types shown in Figure 9, the multiplication factor for the prevailing conditions can be determined.

7. If the pressure read from Figure 8, multiplied by the multiplication factor determined from Figure 9, is 0.1 psi or greater, firing should be postponed.


BEAUREGARD PERKINS, JR.

PAUL H. LORRAIN


WILLIAM H. TOWNSEND

REFERENCES

1. Cox, E. F. et als, "Upper-Atmosphere Temperatures from Helgoland Big Bang", Journal of Meterology, Vol. 6, pp. 300-311, 1949.
2. Ewing, M., and Leet, L. Don "Seismic Propagation Paths." AnAPG Bulletin, 1930.
3. Wiechert, E., and Geiger, L. "Physical Zeits." Vol. 11, pp. 294-311, 1910.
4. Rothwell, P. "Calculation of Sound Rays in the Atmosphere." Journal Acous. Soc. of Am., Vol. 19, pp. 205-221, 1947.
5. Berning, Warren, W. "Investigation of the Propagation of Blast Waves Over Relatively Large Distances and the Damaging Possibilities of Such Propagation." BRL Report No. 675.
6. Dorman, William J., and Brown, J. A. "Meteorological Focusing of Sound and Blast Waves and Its Prediction by Analogue Techniques." BRL Report No. 1014.

APPENDIX A

APPROXIMATIONS IN ANALOGUE

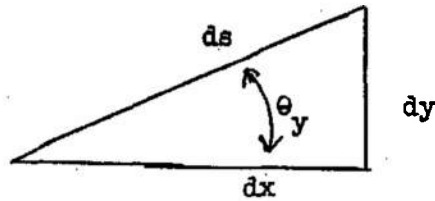
SOLUTION OF RAY PATHS

The following was furnished by Mr. DeBow Owen of Piedmont Division, Sperry-Rand Corporation, Charlottesville, Virginia.

Since the Ray Tracer computing system integrates in the time domain, y must be expressed as a function of time;

$$\dot{y} = \frac{dy}{dt} = \frac{dy}{ds} \frac{ds}{dt} = V_y \sin \theta_y \quad (1)$$

in which θ_y = angle between the ray and the horizontal and V_y is the velocity of sound, at altitude Y .



$$\begin{aligned} \dot{y} &= \frac{d}{dt} (V_y \sin \theta_y) \\ &= \frac{1}{C} (\cos^2 \theta_y - \sin^2 \theta_y) \frac{d\theta_y}{dt} \\ &= \frac{1}{C} (\cos 2\theta_y) \frac{d\theta_y}{dt} \end{aligned} \quad (2)$$

Since $\cos \theta_y = CV_y$, $\frac{d\theta_y}{dt} = -CV_y \frac{dV_y}{dy}$

and substituting in (2)

$$\dot{y} = -V_y (\cos 2\theta_y) \frac{dV_y}{dy} \quad (3)$$

In the Ray Tracer the assumption is made that the horizontal distance traveled is equal to a constant average velocity times the travel time,

$$\text{i.e., } x = V_{av} t, \quad V_{av} = \text{constant}$$

$$\text{then } \dot{y} = \frac{dy}{dx} \frac{dx}{dt} = v_{av} \tan \theta_y \quad (4)$$

$$\text{and } \dot{y} = v_{av} \sec^2 \theta_y \frac{d\theta_y}{dt} \quad (5)$$

$$\text{Now } \theta_y = \cos^{-1} (C) (v_y)$$

$$\begin{aligned} \text{and } \frac{d\theta_y}{dt} &= - \frac{C}{\sin \theta_y} \frac{dv_y}{dt} \\ &= \frac{-C}{\sin \theta_y} \frac{dv_y}{dy} \frac{dy}{dx} \frac{dx}{dt} \\ &= \frac{-C}{\sin \theta_y} (\tan \theta_y) (v_{av}) \frac{dv_y}{dy} \\ &= \frac{-C v_{av}}{\cos \theta_y} \frac{dv_y}{dy} \end{aligned}$$

$$\text{and } \ddot{y} = \frac{-C v_{av}^2}{\cos \theta_y} \sec^2 \theta_y \frac{dv_y}{dy} \quad (6)$$

$$\begin{aligned} \text{and again since } \frac{C}{\cos \theta_y} &= \frac{1}{v_y} \\ \ddot{y} &= \frac{-v_{av}^2}{v_y \cos^2 \theta_y} \frac{dv_y}{dy} \quad (7) \end{aligned}$$

The gradients commonly experienced in the lower atmosphere are small (0 to .040 ft/sec/ft.) and persist for only a few thousand feet. For this reason, the rays that return to the surface will traverse a path, the direction of which will have a maximum inclination to the horizontal less than 12 degrees. Therefore a further approximation has been made that $\cos^2 \theta_y = 1$.

$$\text{Then } \ddot{y} = \frac{-v_{av}^2}{v_y} \frac{dv_y}{dy} \quad (8)$$

Equation (8) is used in the ray tracer in lieu of the more precise equation (21) of the text. A comparison of the exact solution of these two equations will provide an estimate of the error caused by the approximations. When the initial slope of the ray is eleven degrees, the difference between the true and the approximate maximum height reached by the ray is 1.6 per cent. The difference in the true range and the approximate range is 1.2 per cent. These differences are insignificant.

APPENDIX B

TYPICAL VERTICAL VELOCITY GRADIENTS

In the following pages there is presented a set of gradients which are typical of conditions found at Aberdeen Proving Ground over a two year period. The velocity at each altitude was determined from the temperature and wind velocity.

With each velocity versus altitude curve the resulting sound ray paths, as computed on the Sperry-Rand Electronic Ray Plotter, are shown.

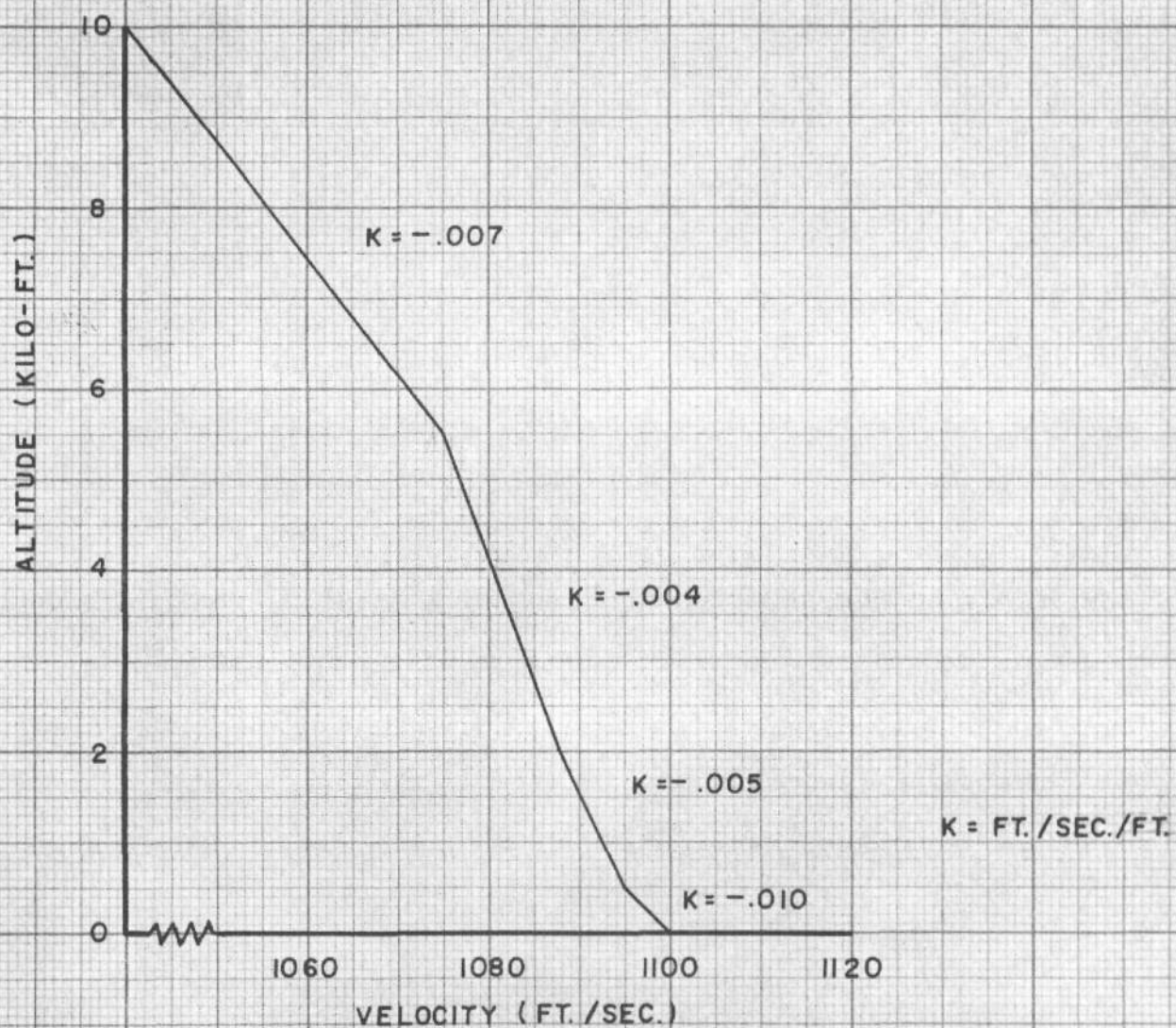
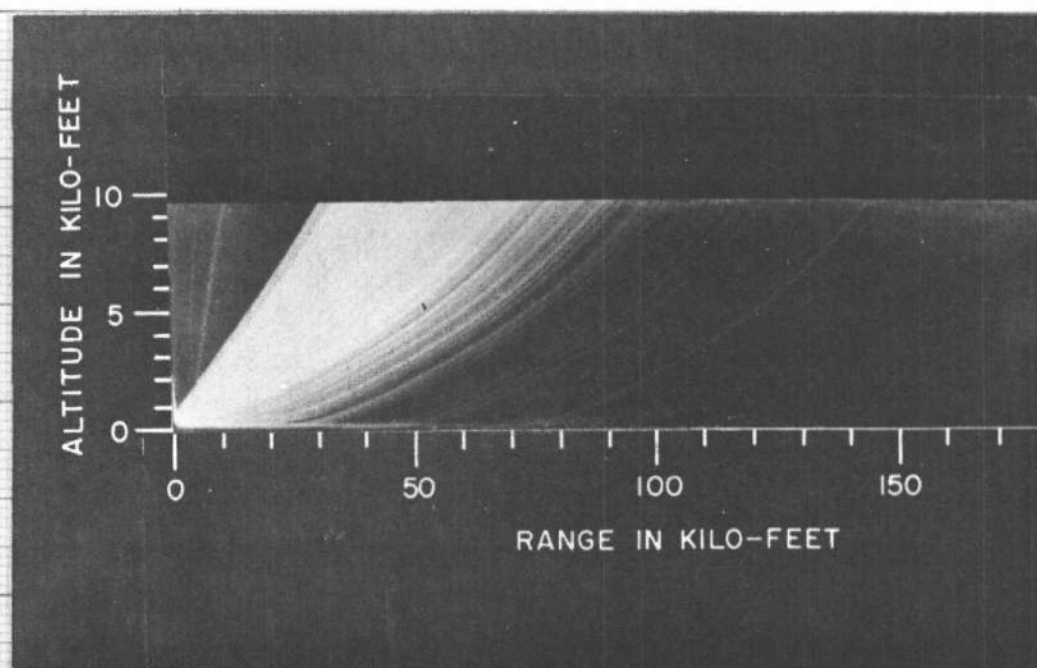


FIGURE 1

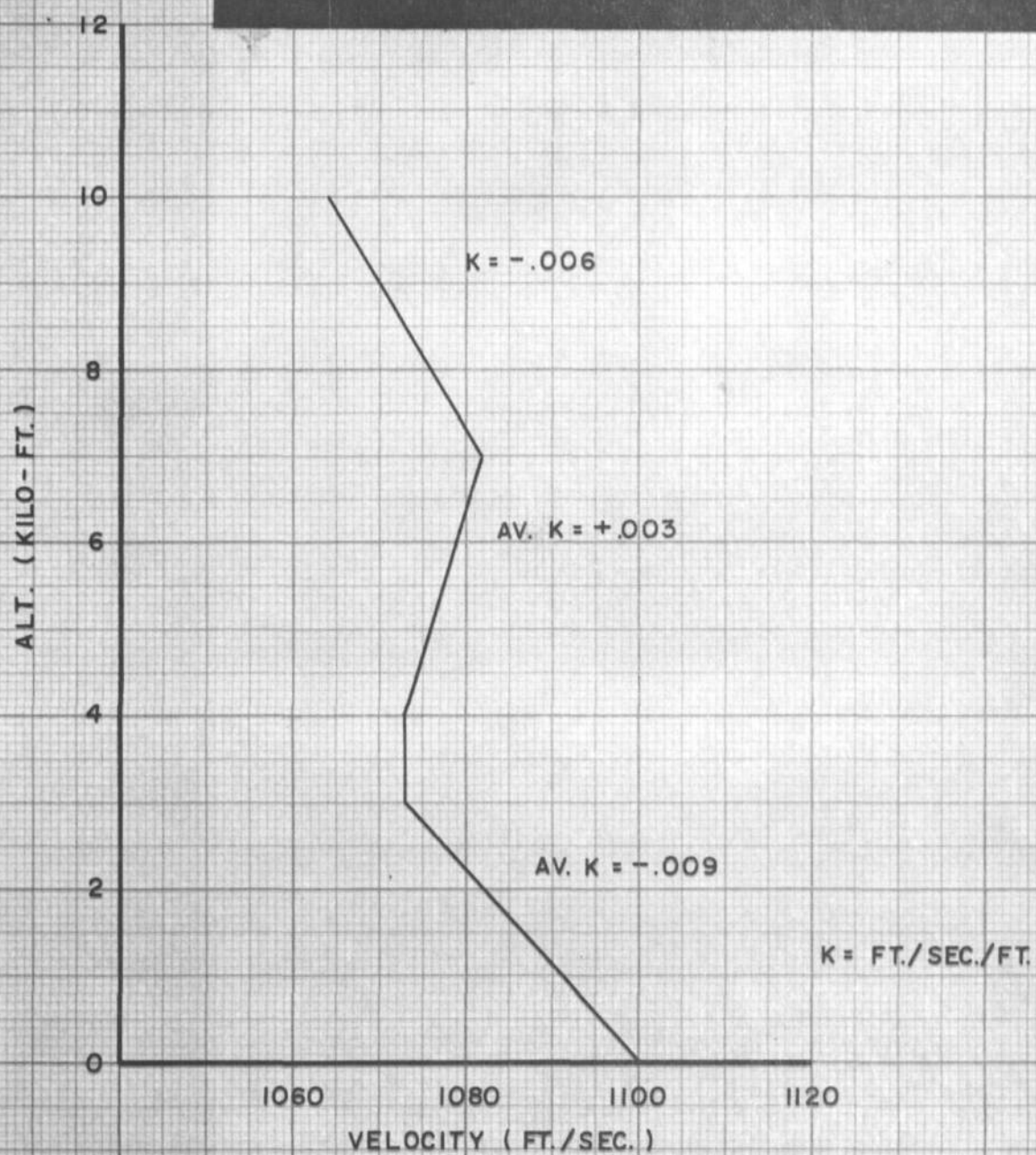
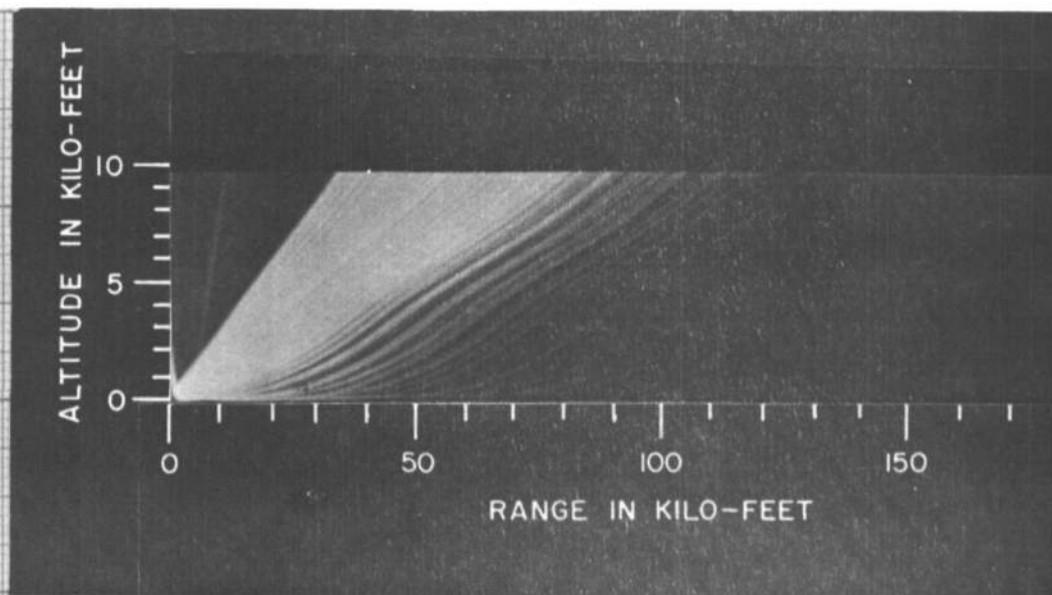


FIGURE 2

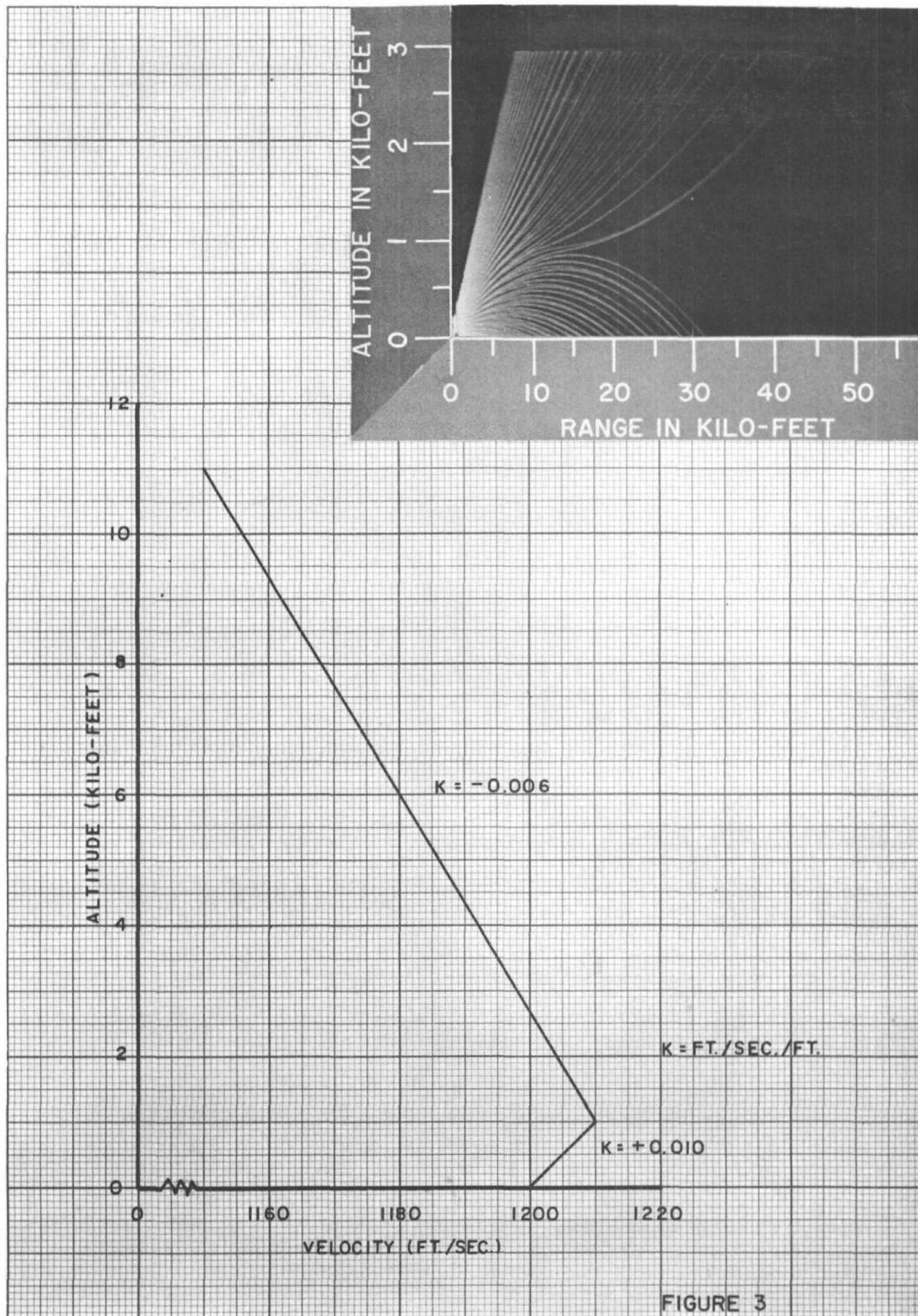


FIGURE 3

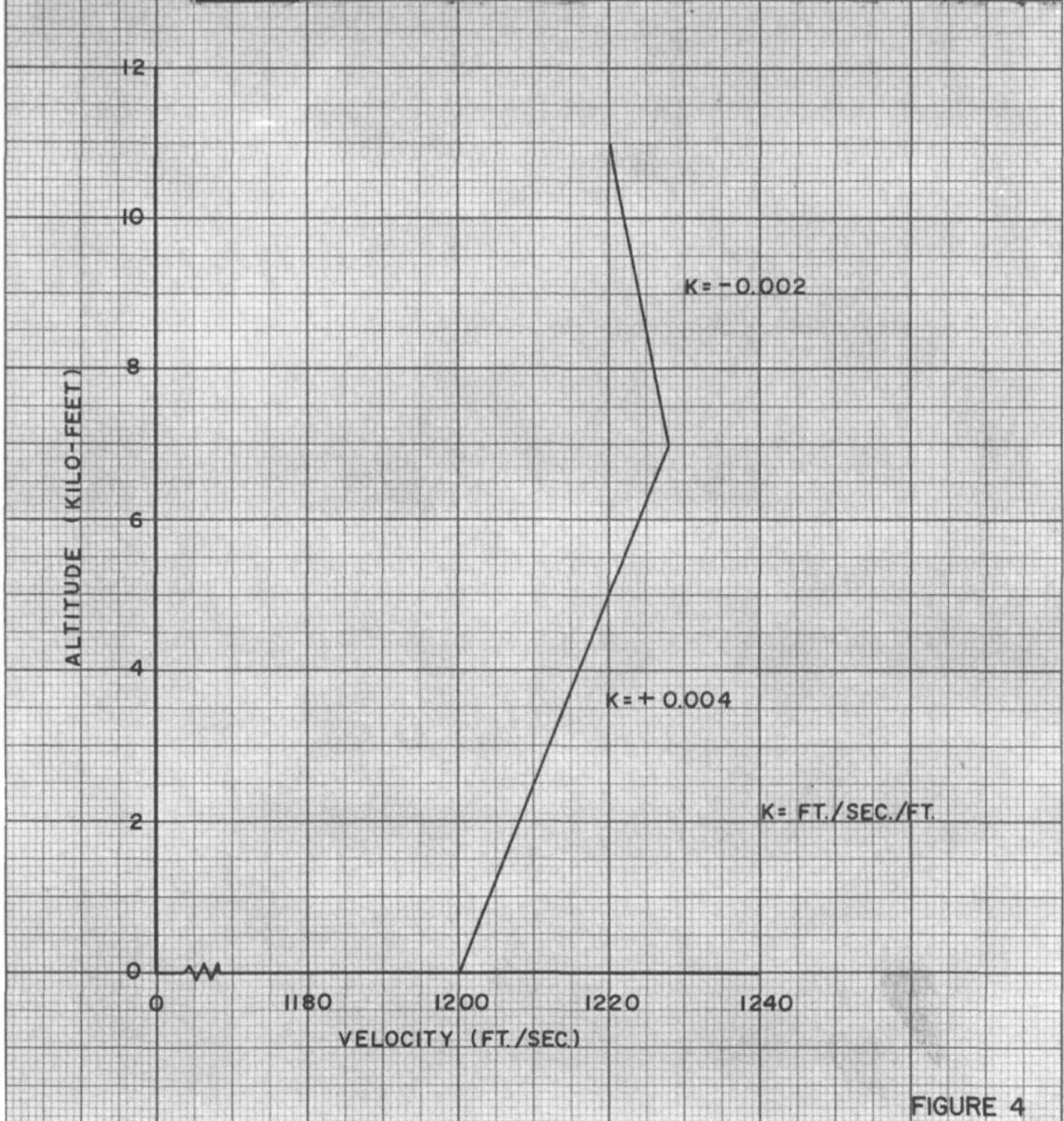
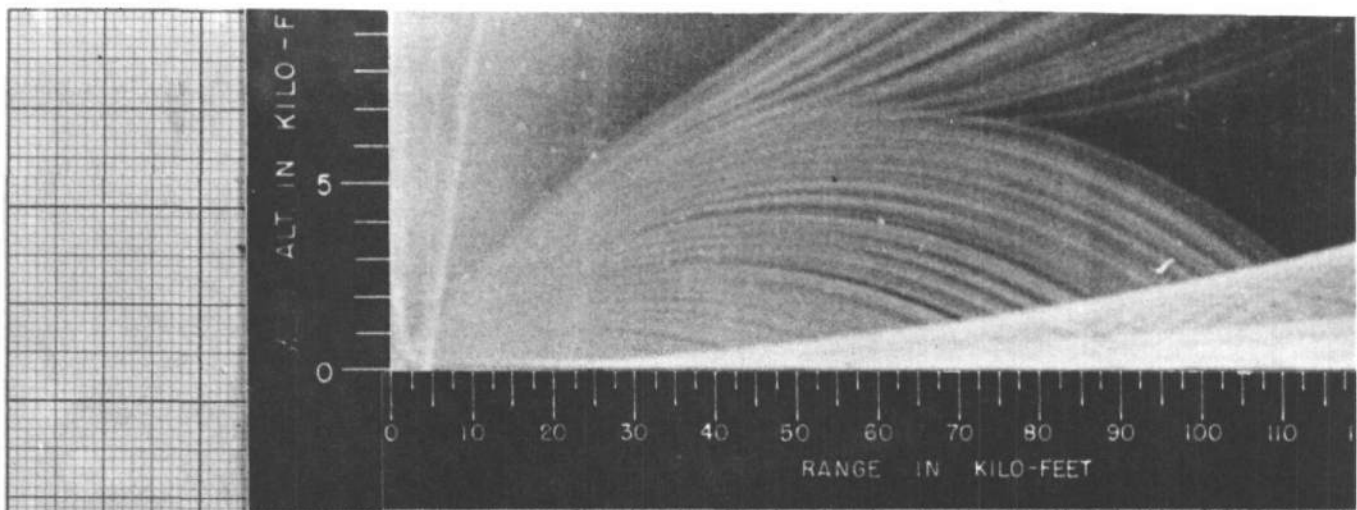


FIGURE 4

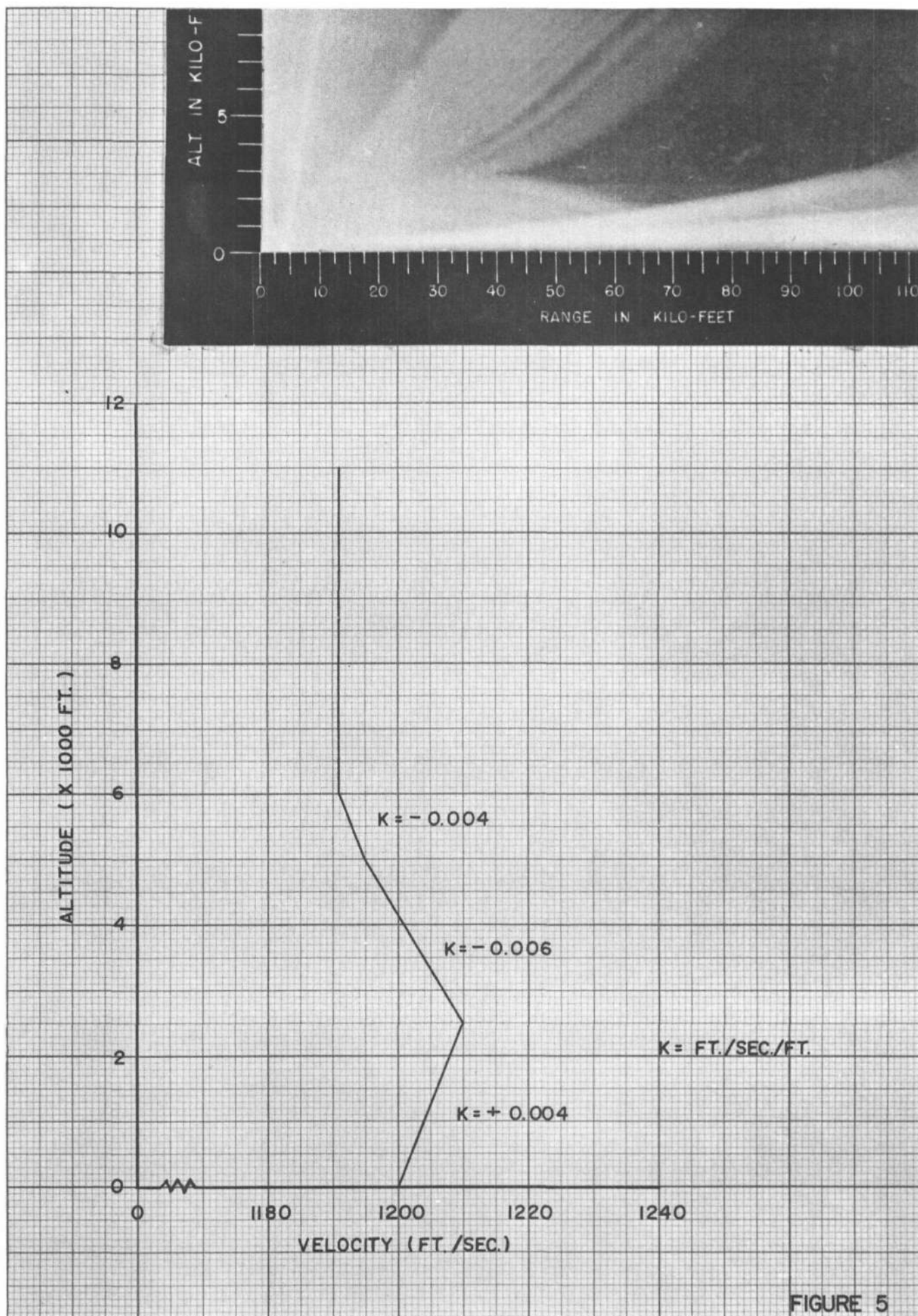


FIGURE 5

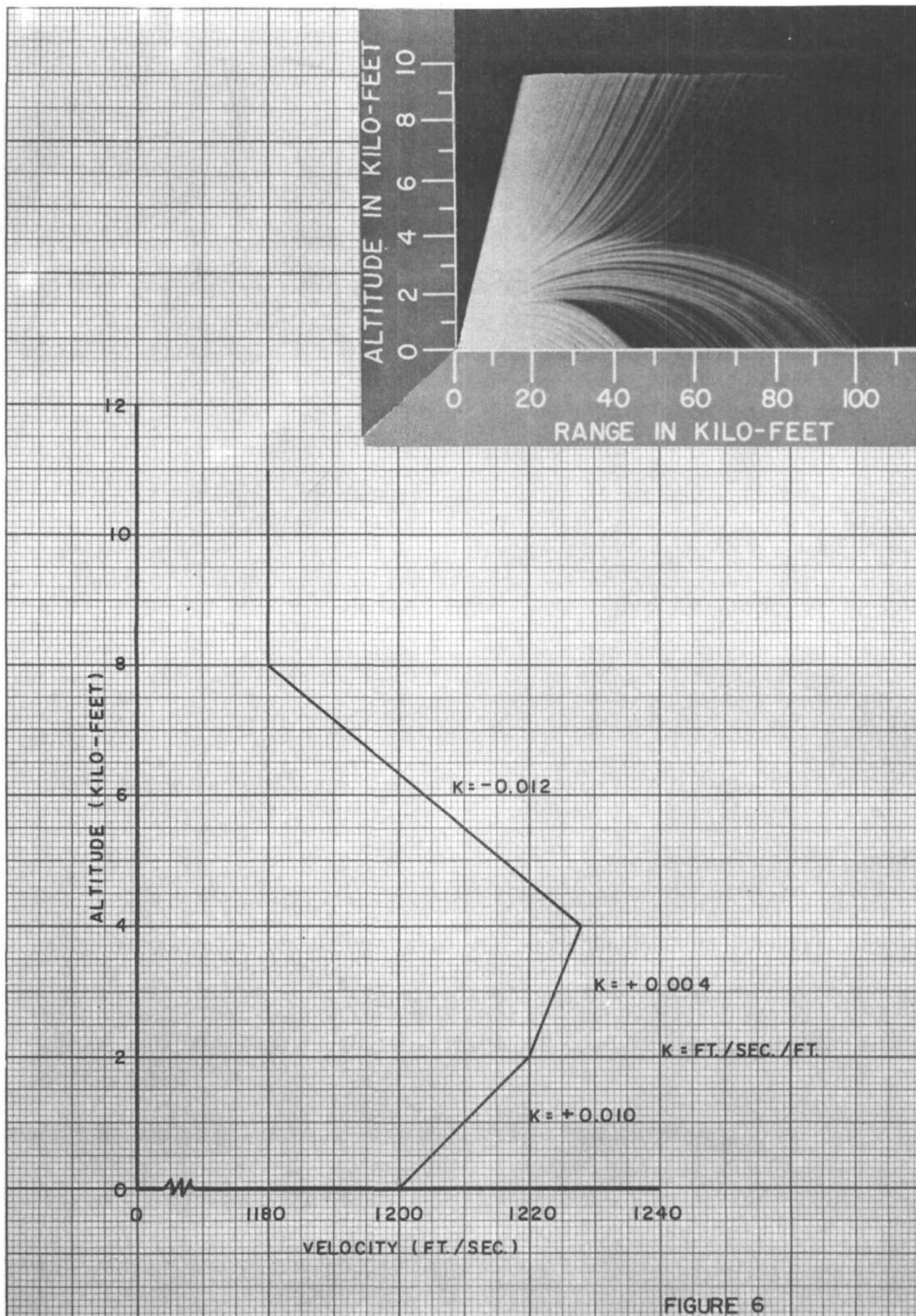


FIGURE 6

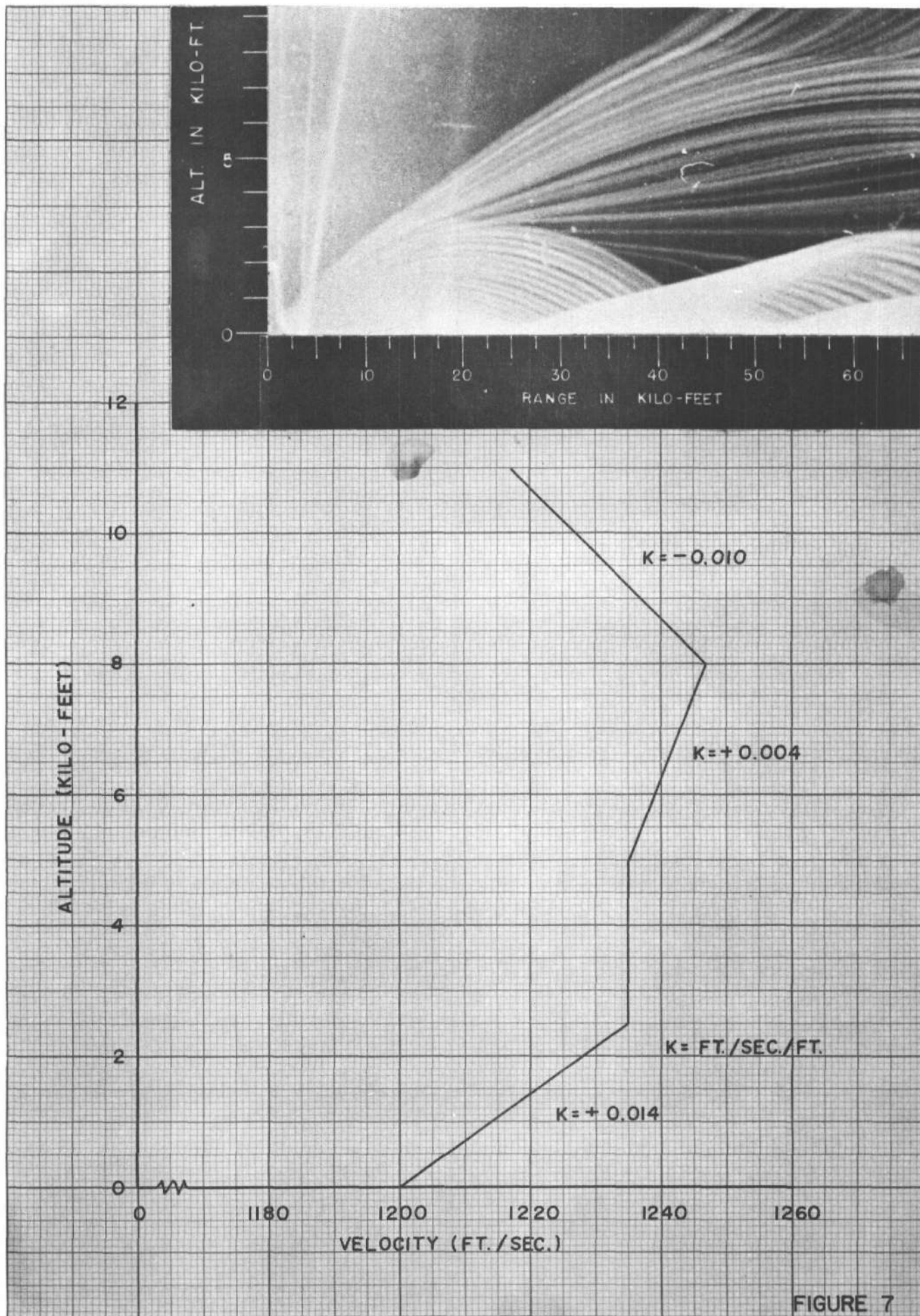


FIGURE 7

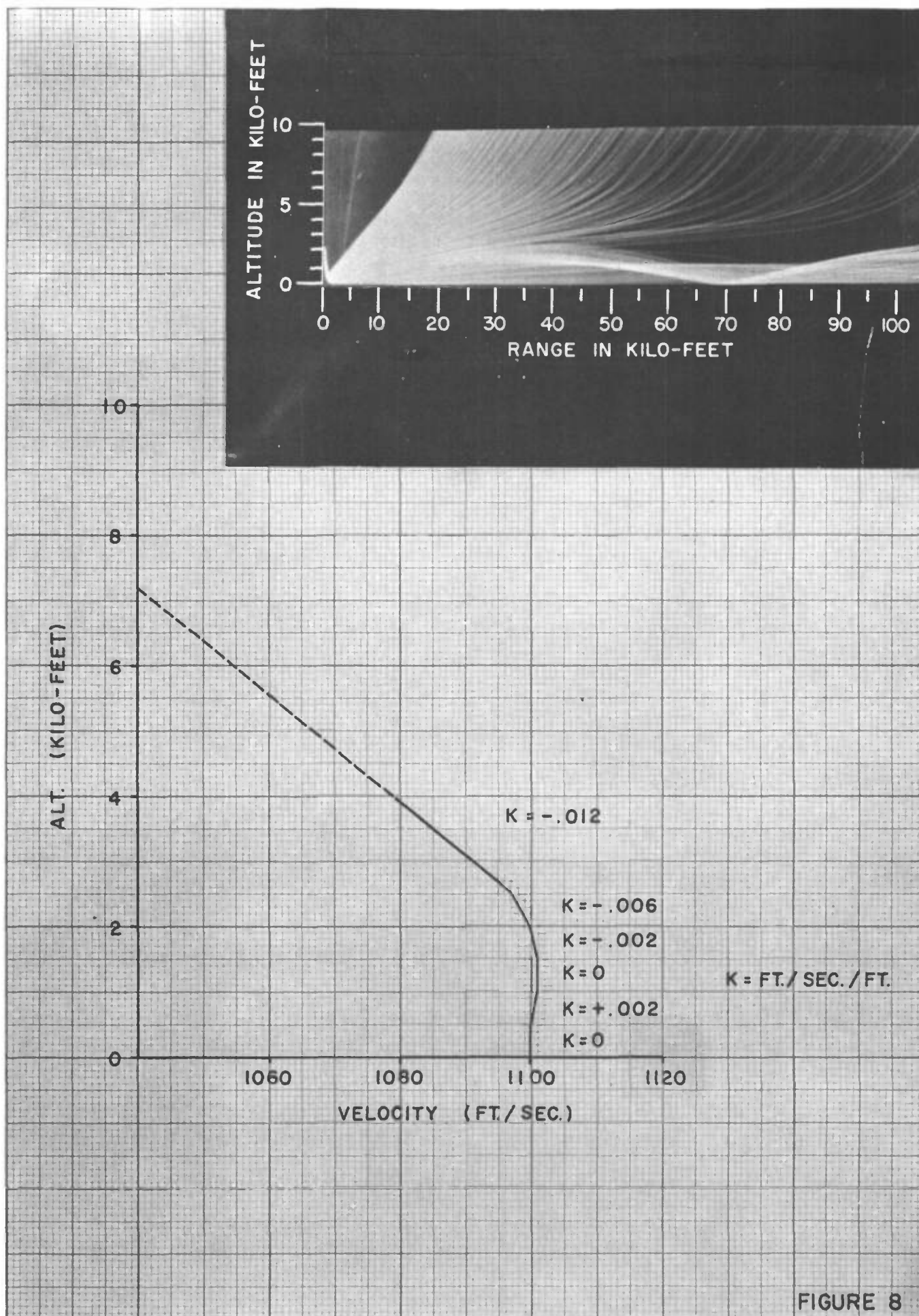


FIGURE 8

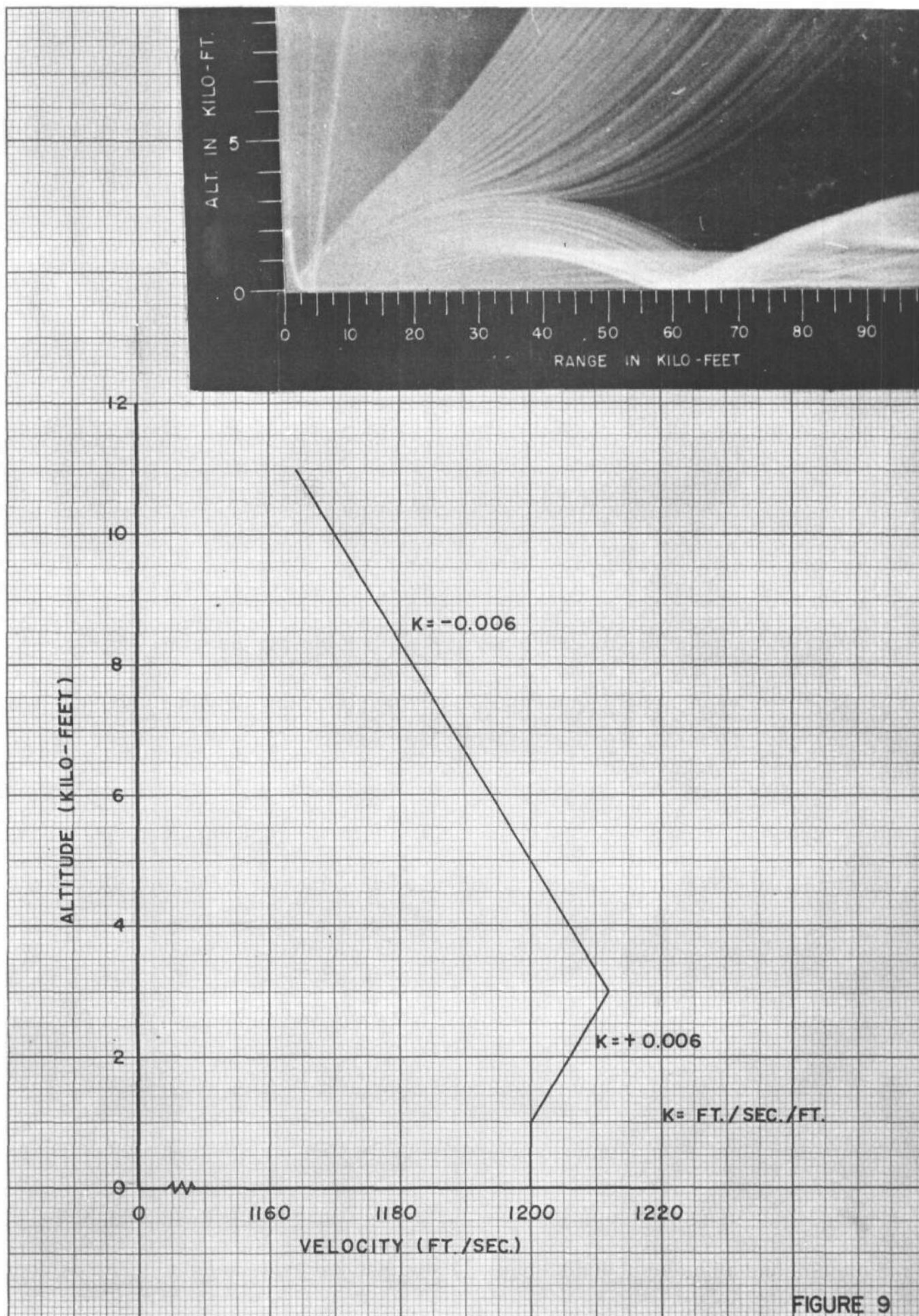


FIGURE 9

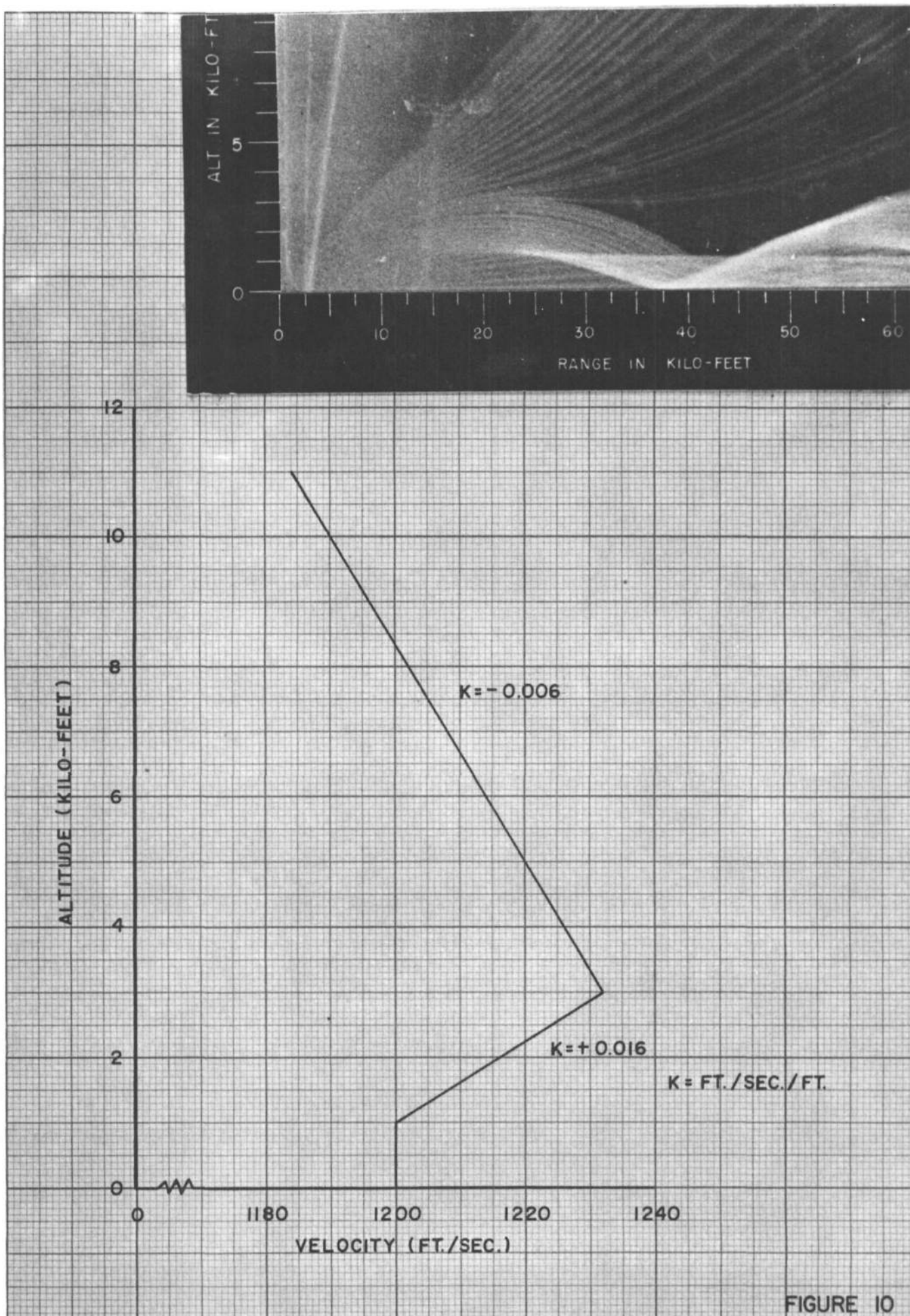
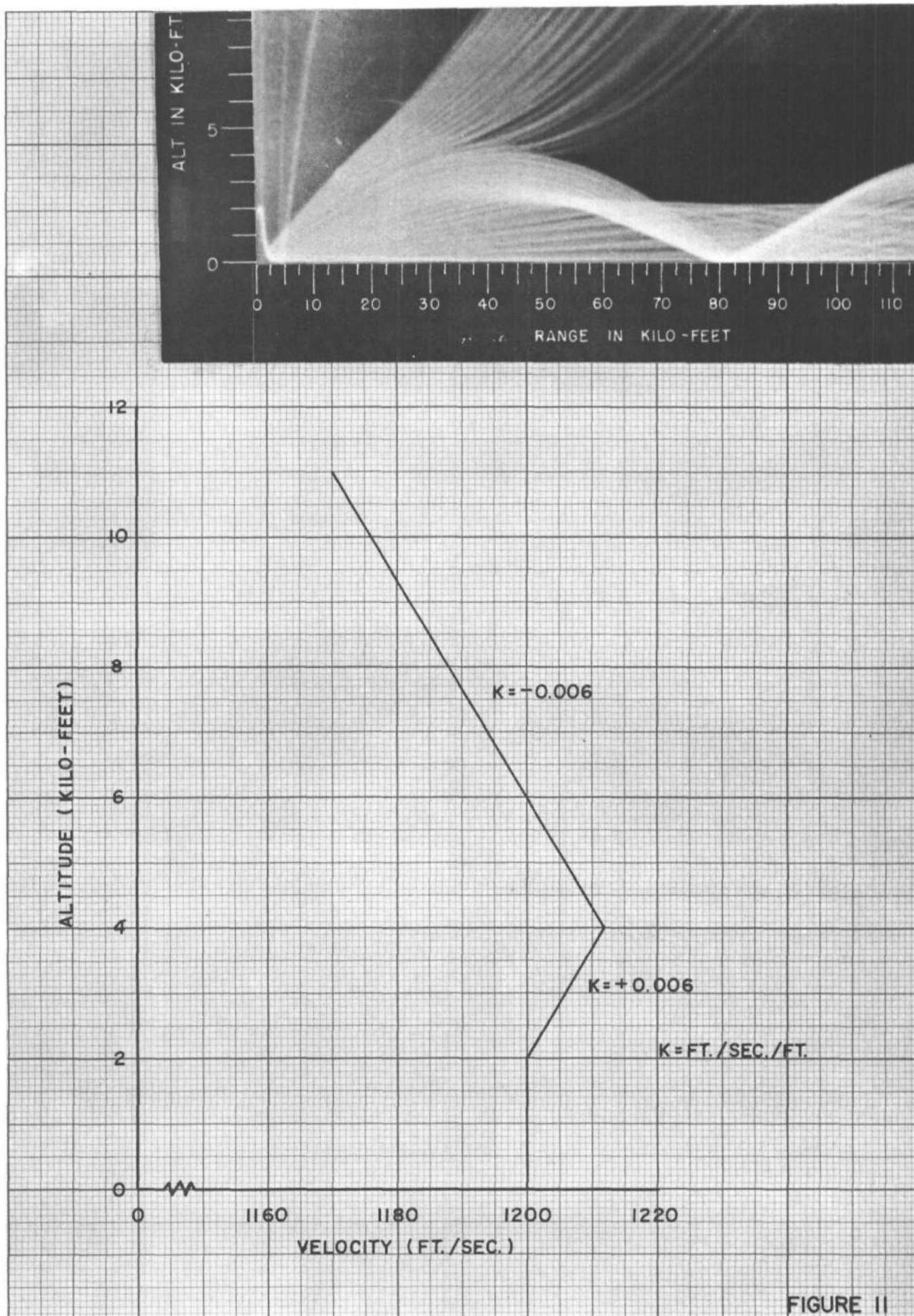


FIGURE 10



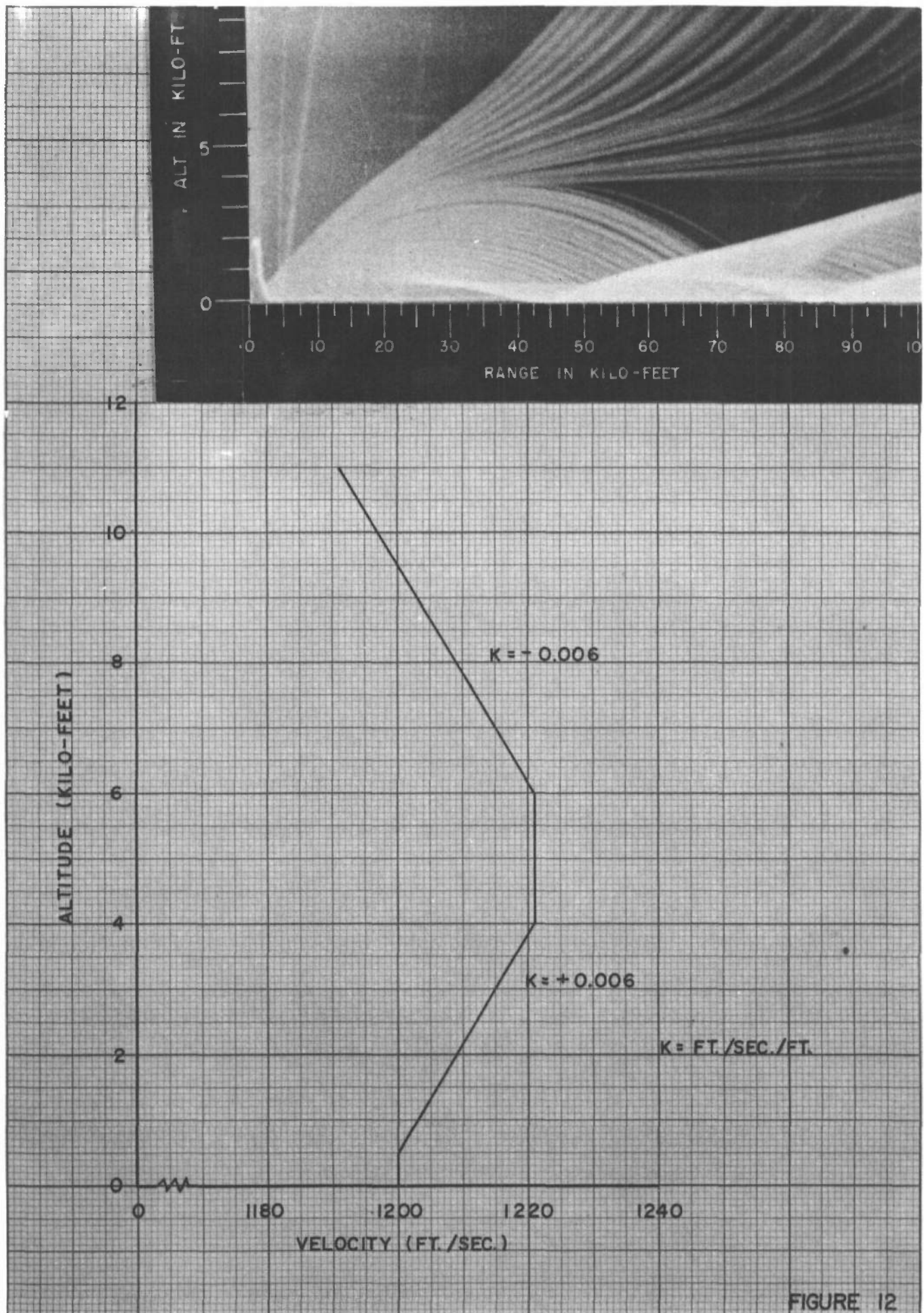


FIGURE 12

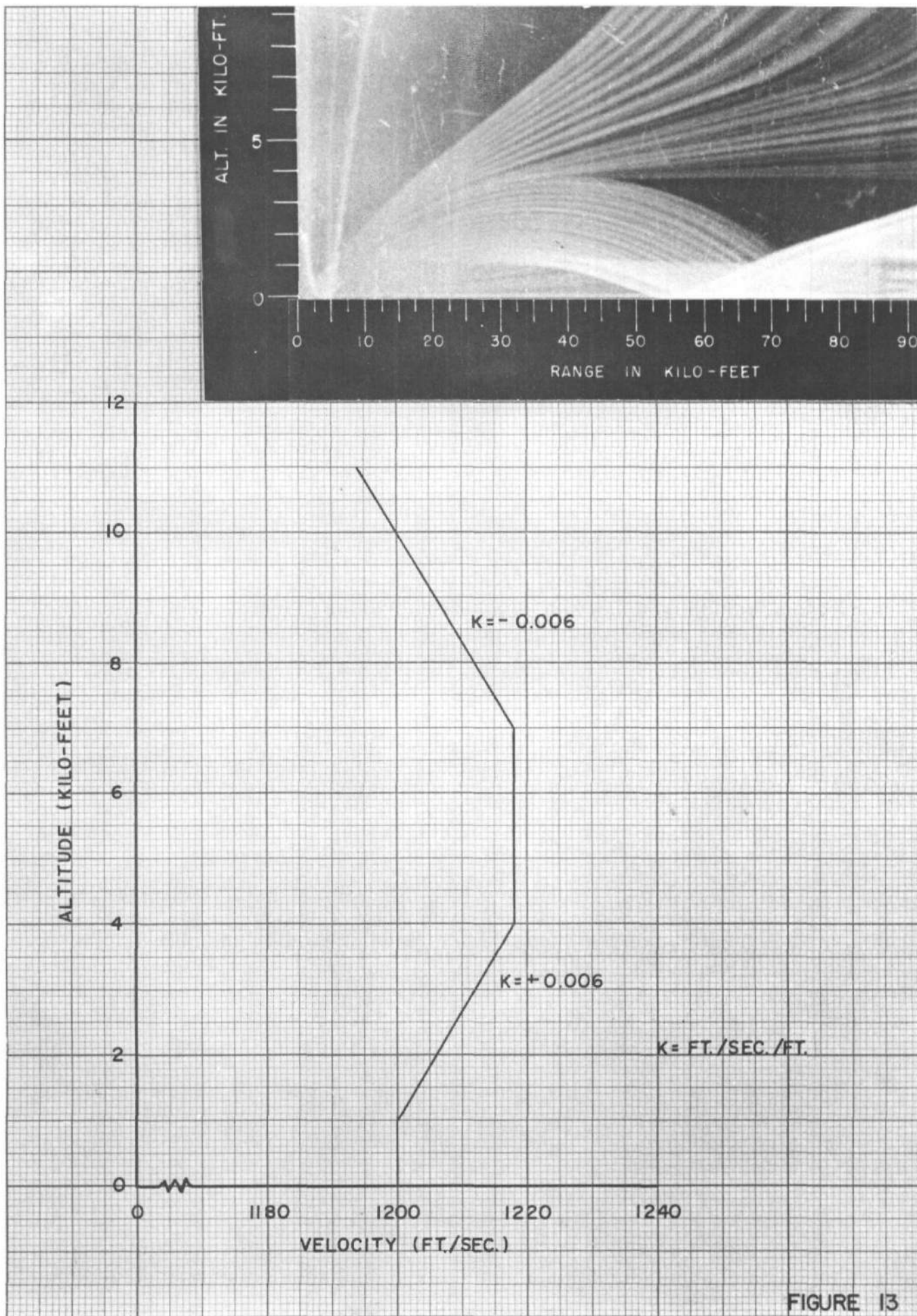
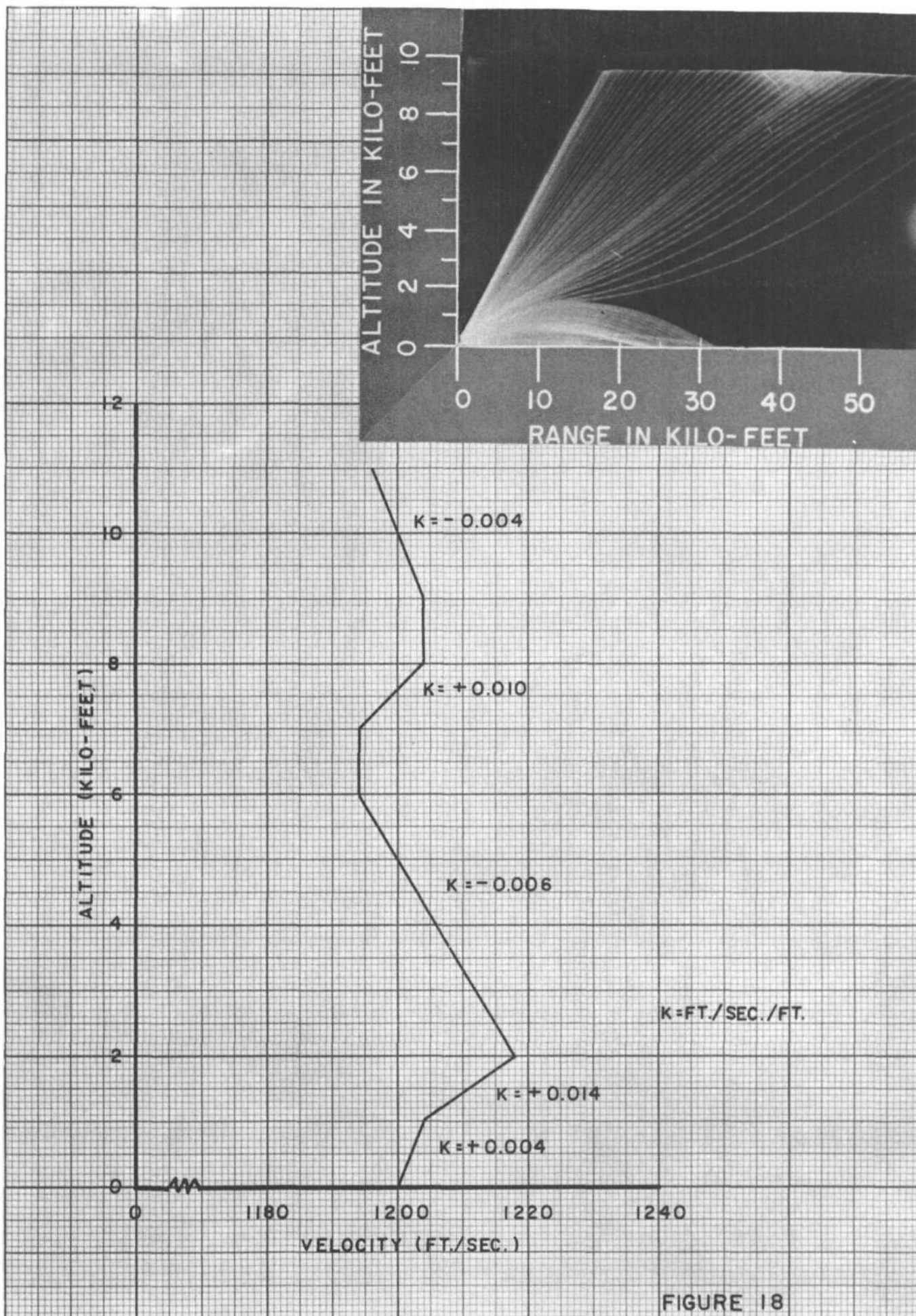


FIGURE 13



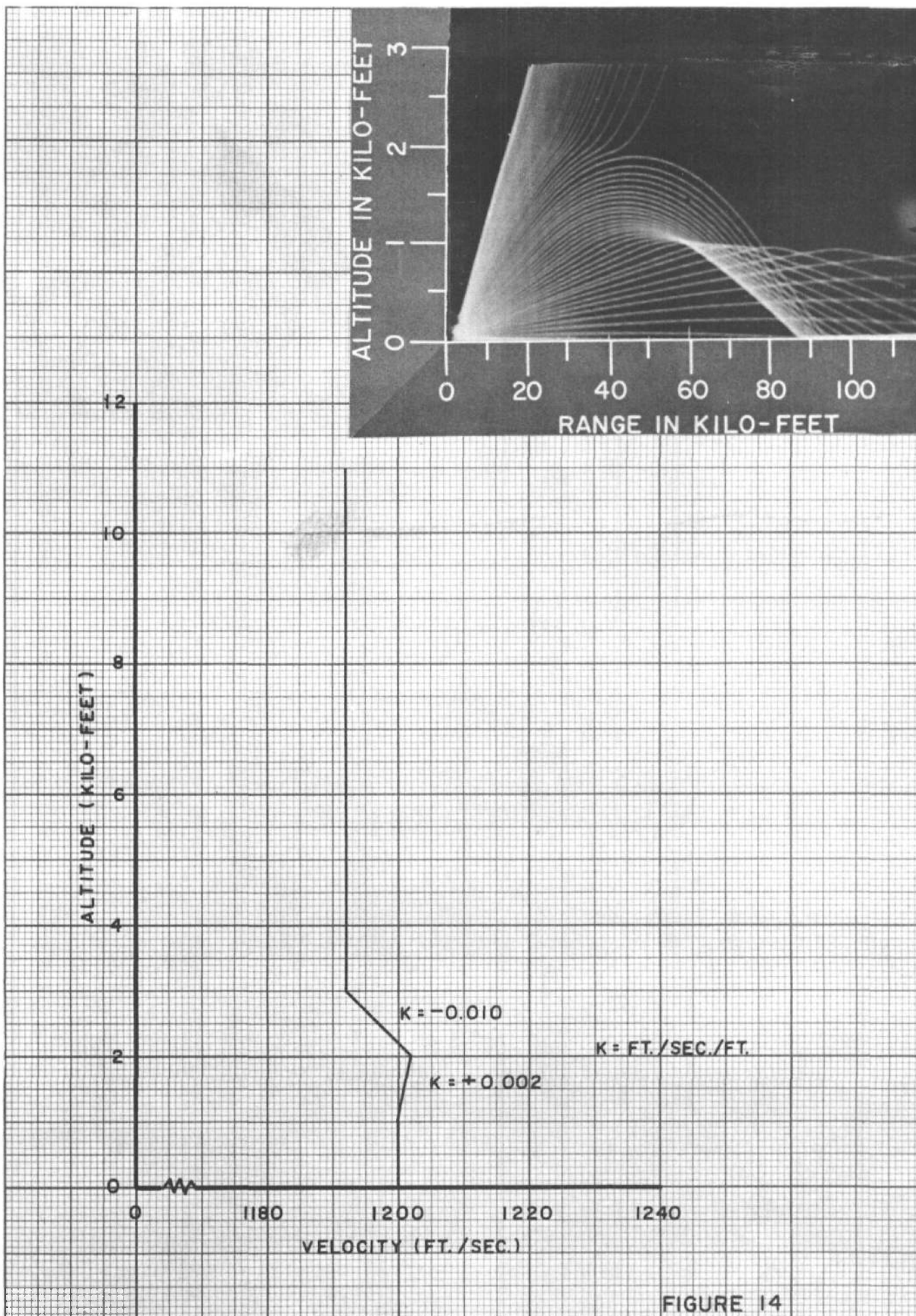


FIGURE 14

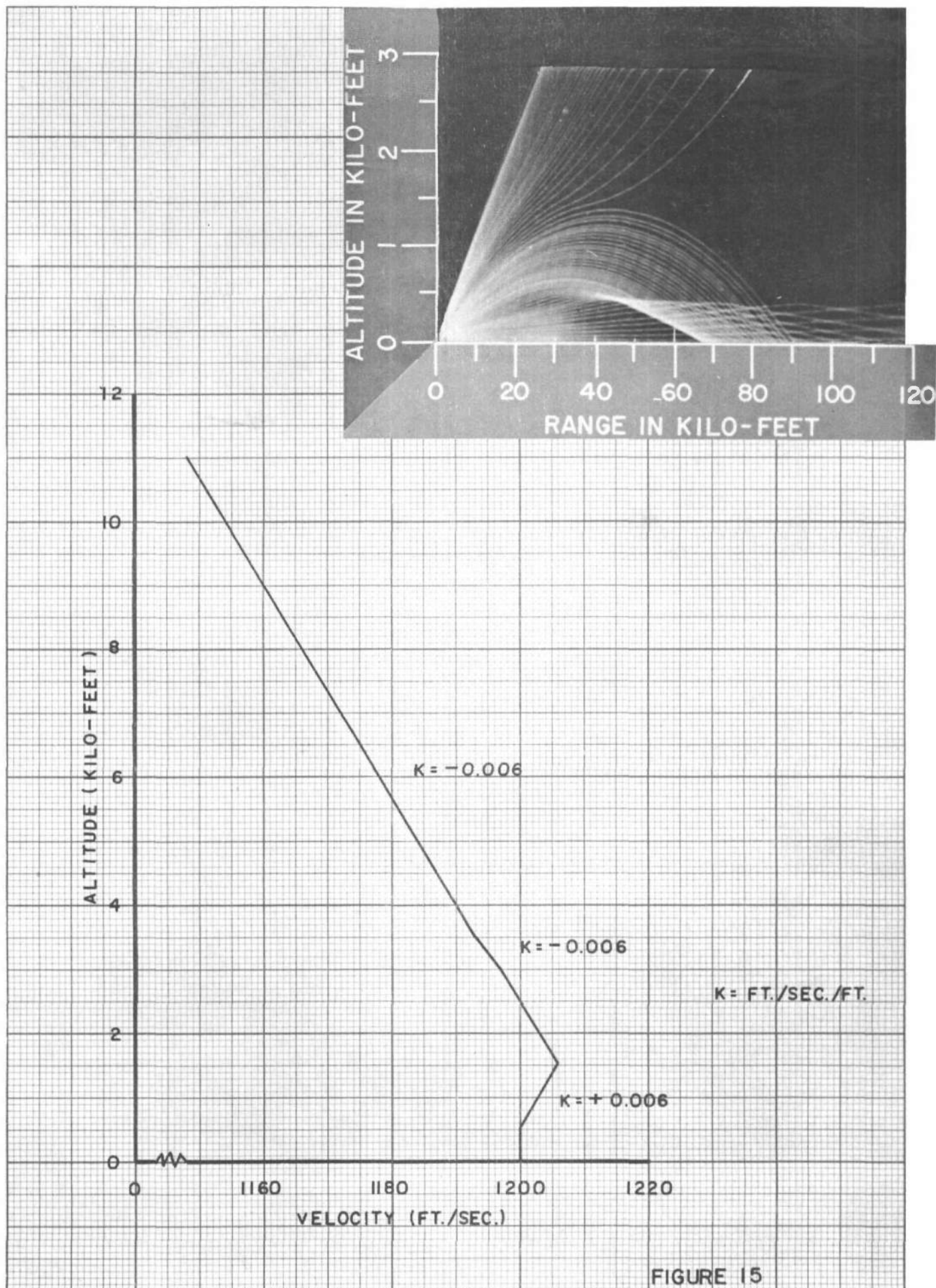


FIGURE 15

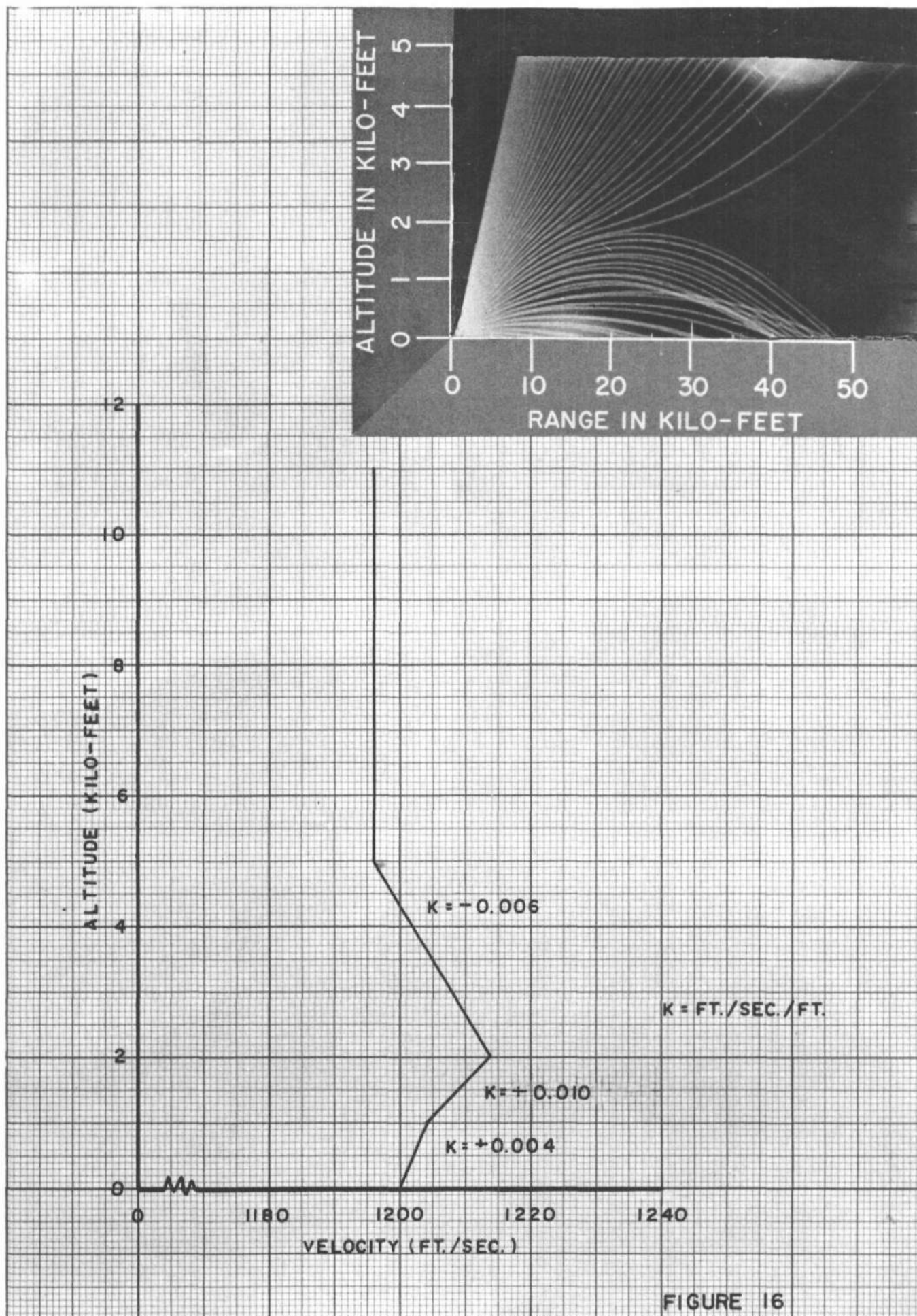


FIGURE 16

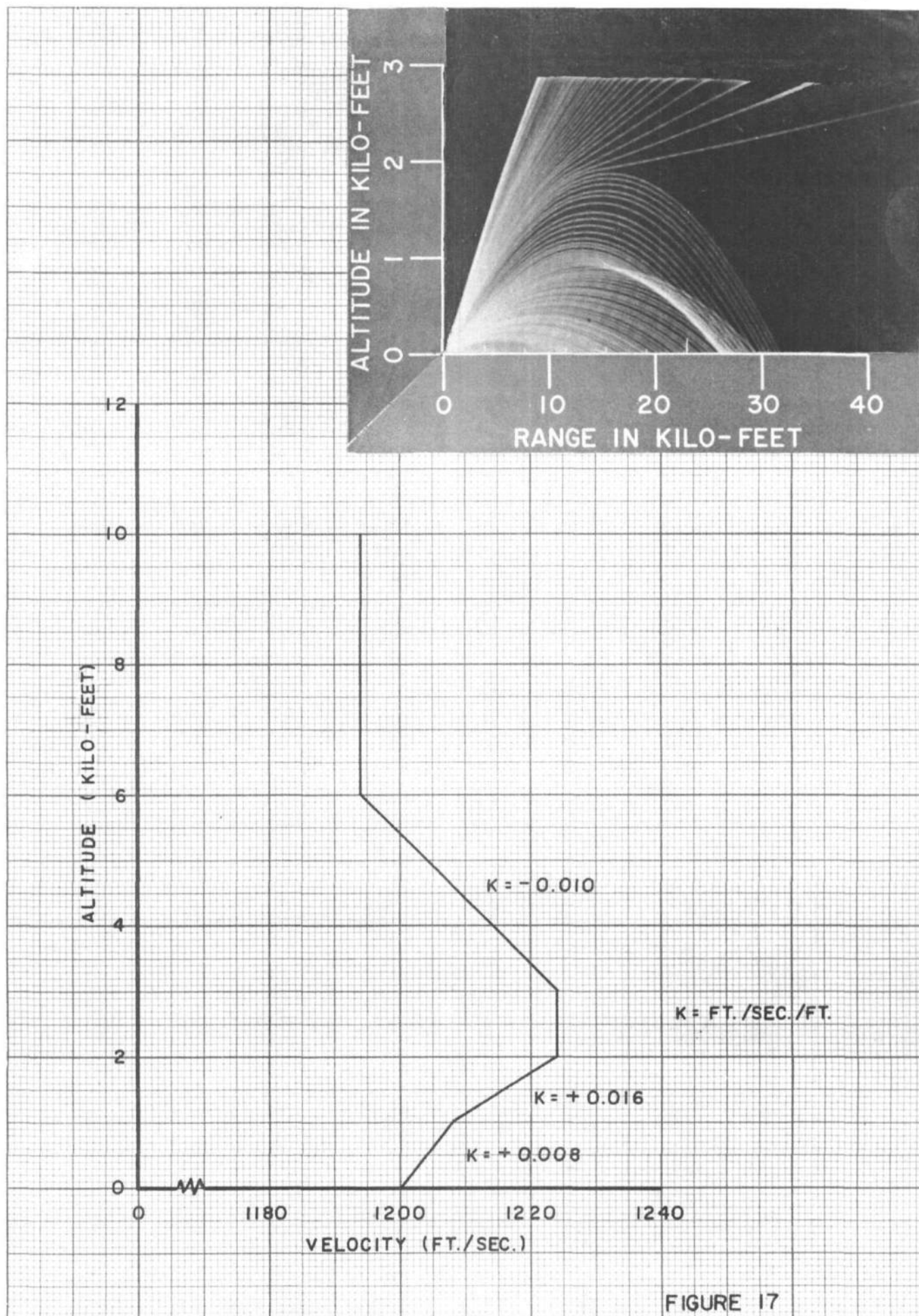


FIGURE 17

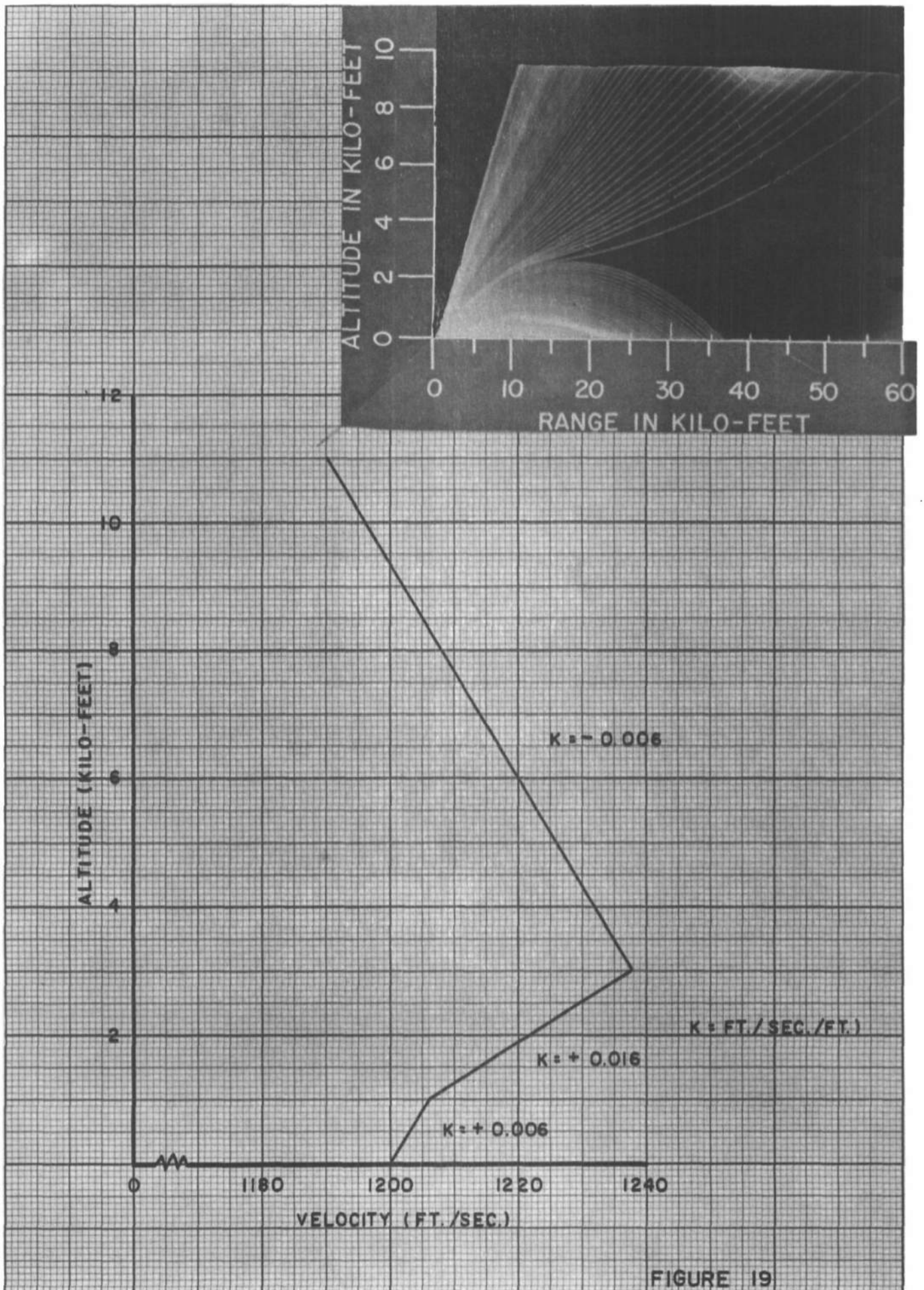


FIGURE 19

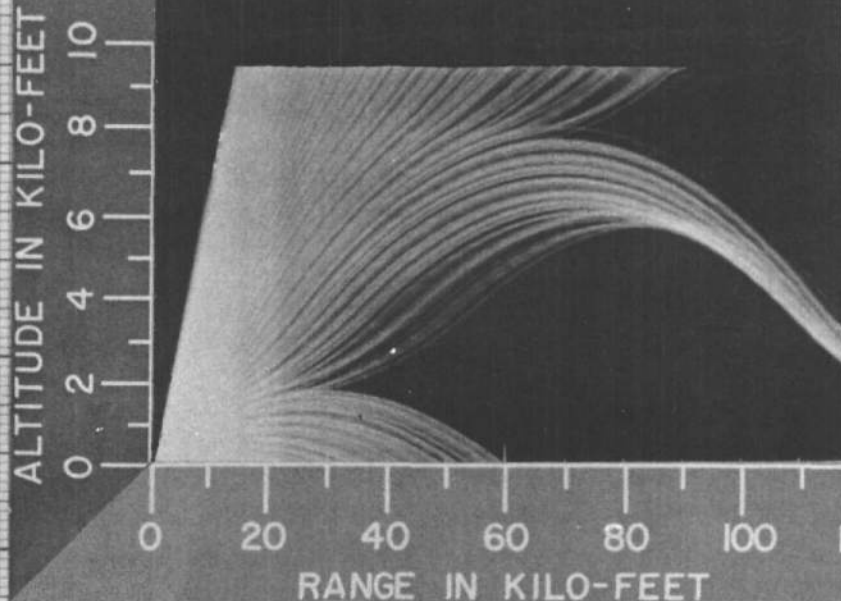
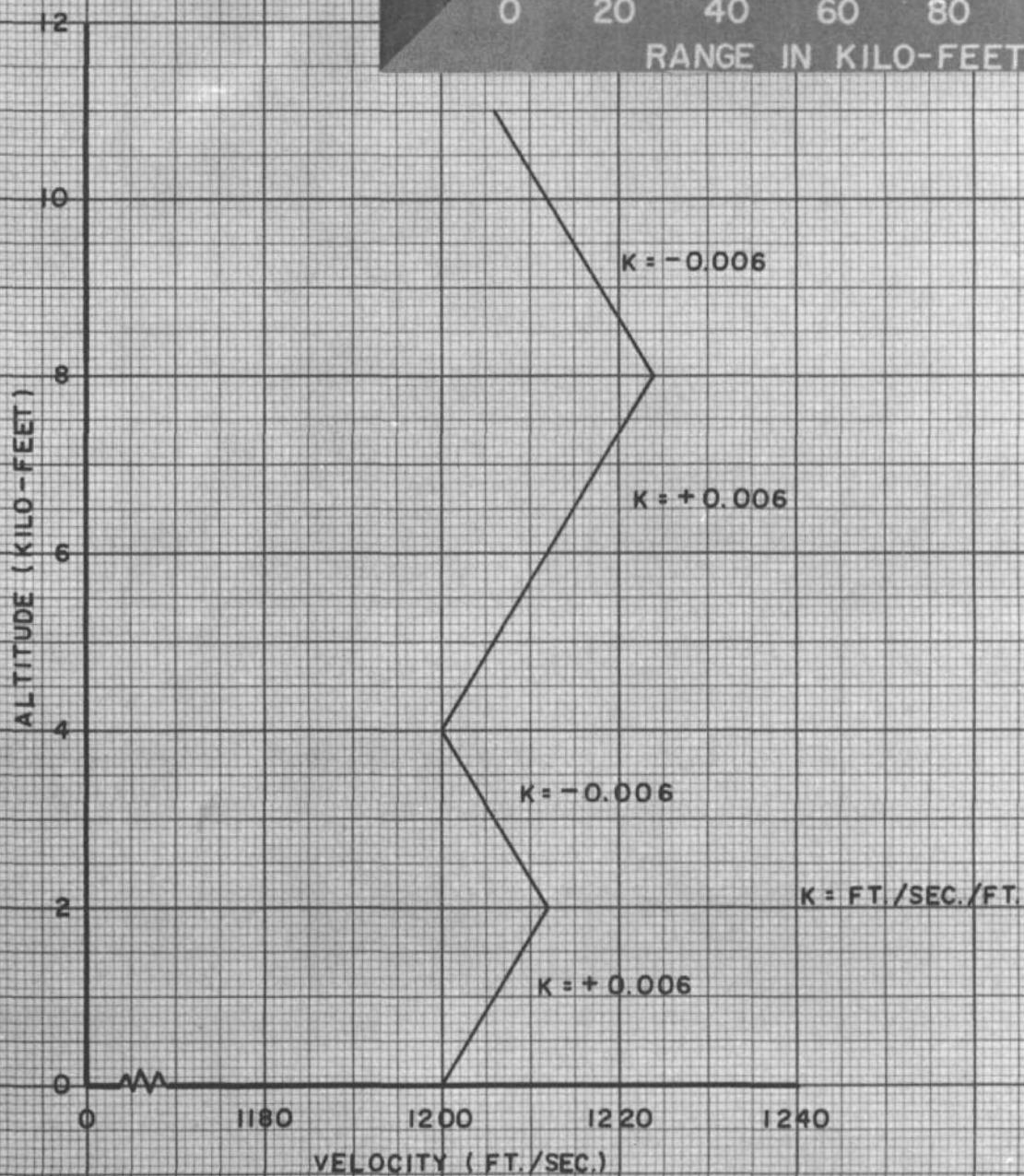


FIGURE 20

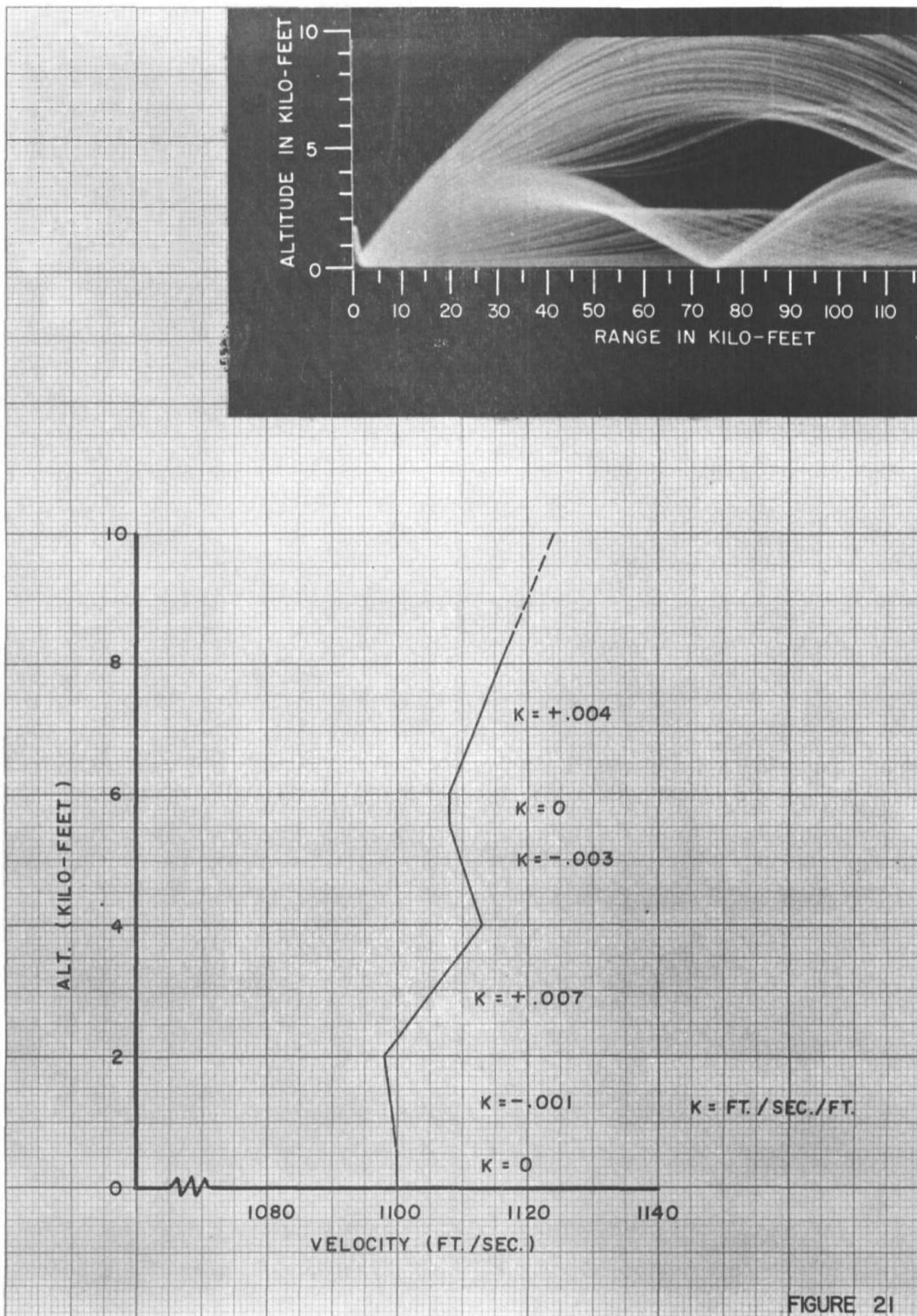


FIGURE 21

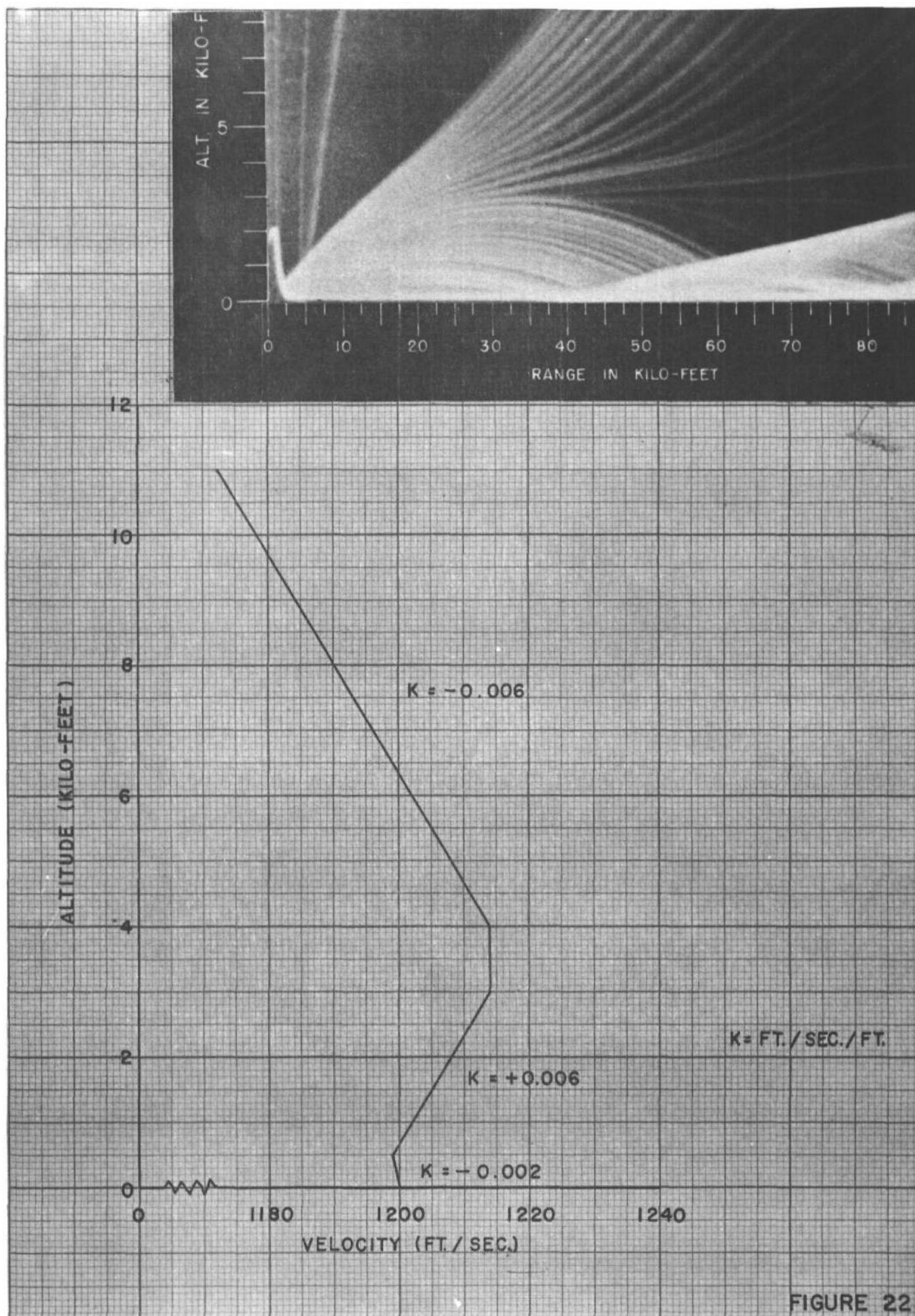


FIGURE 22

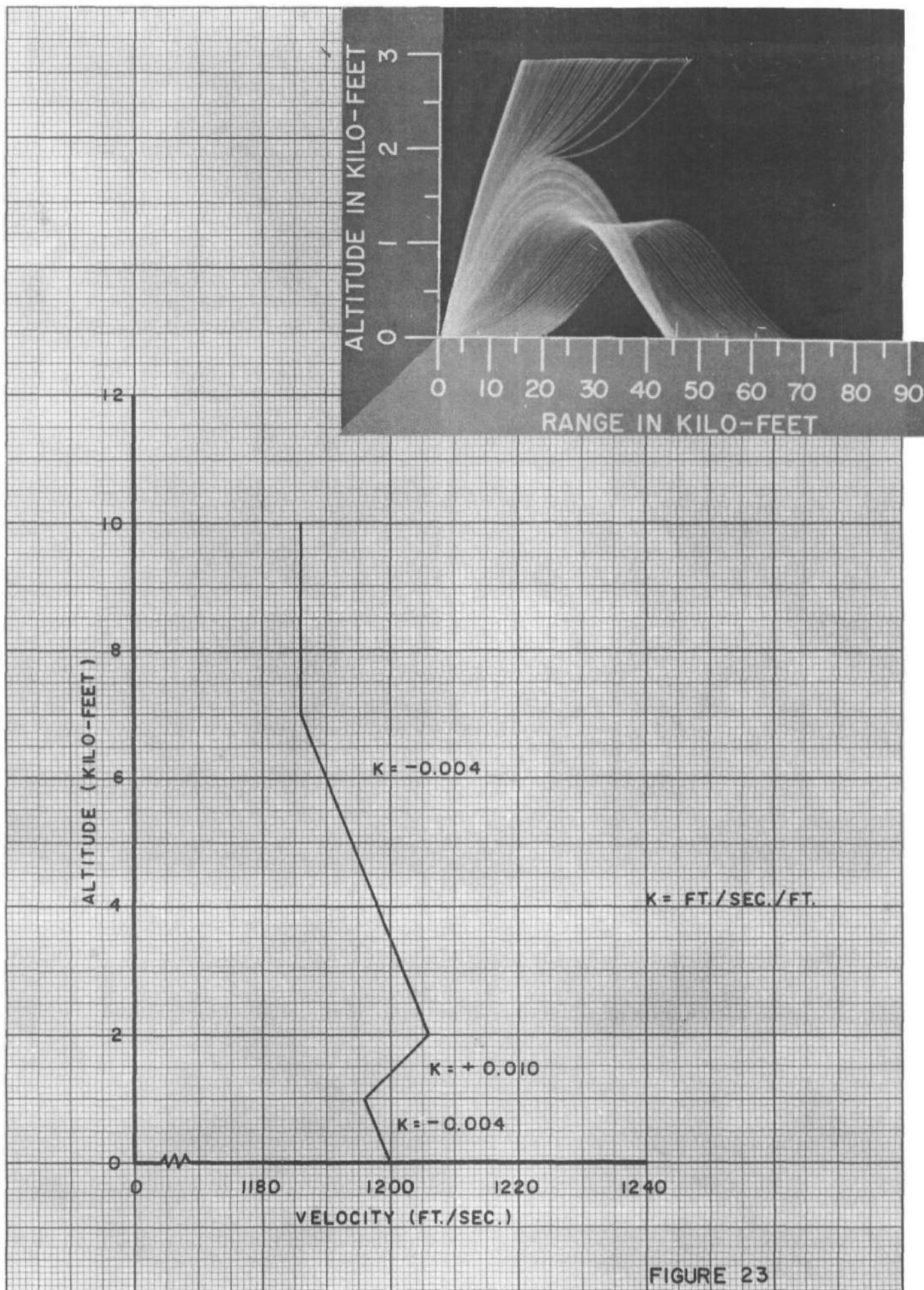


FIGURE 23

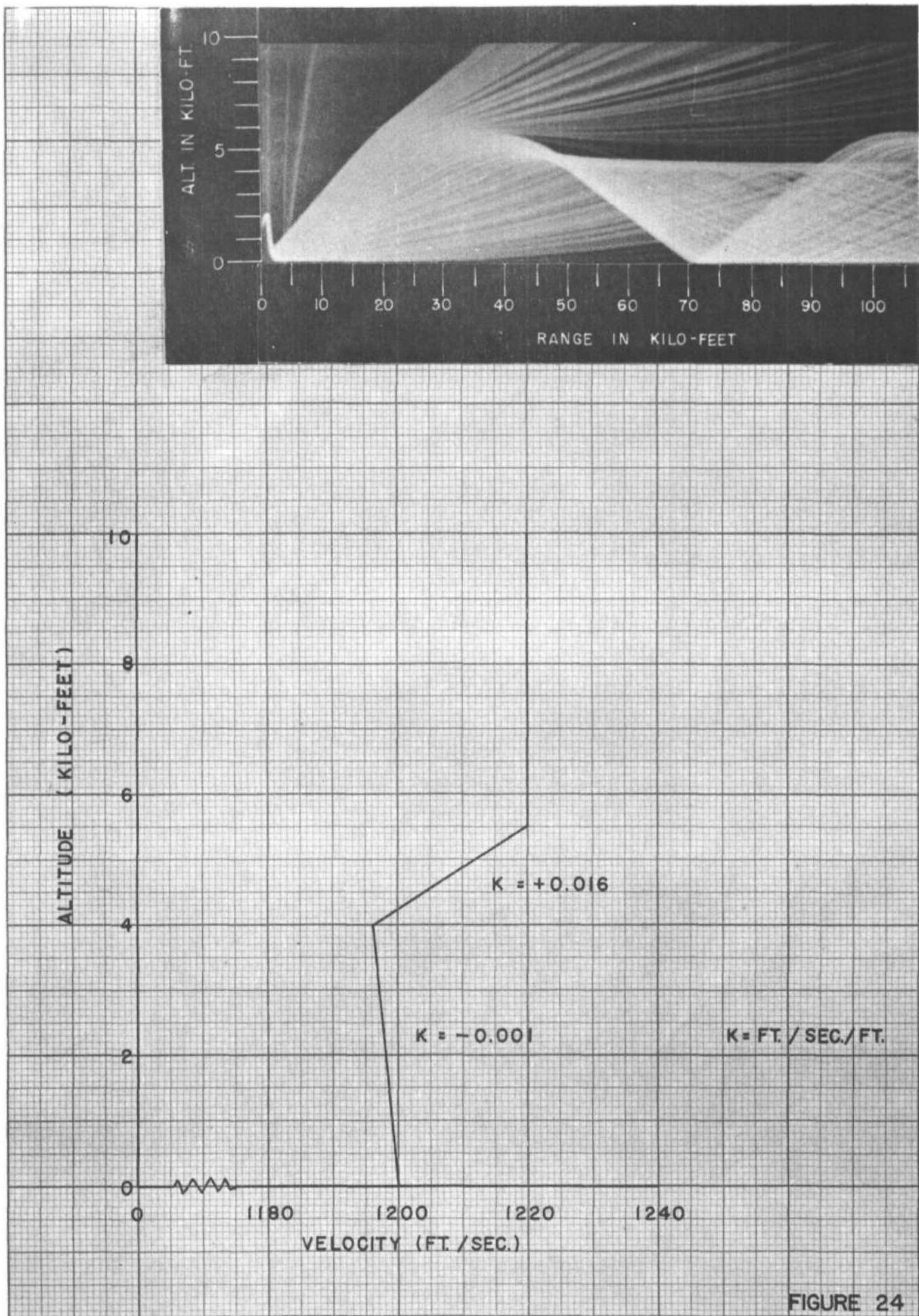


FIGURE 24

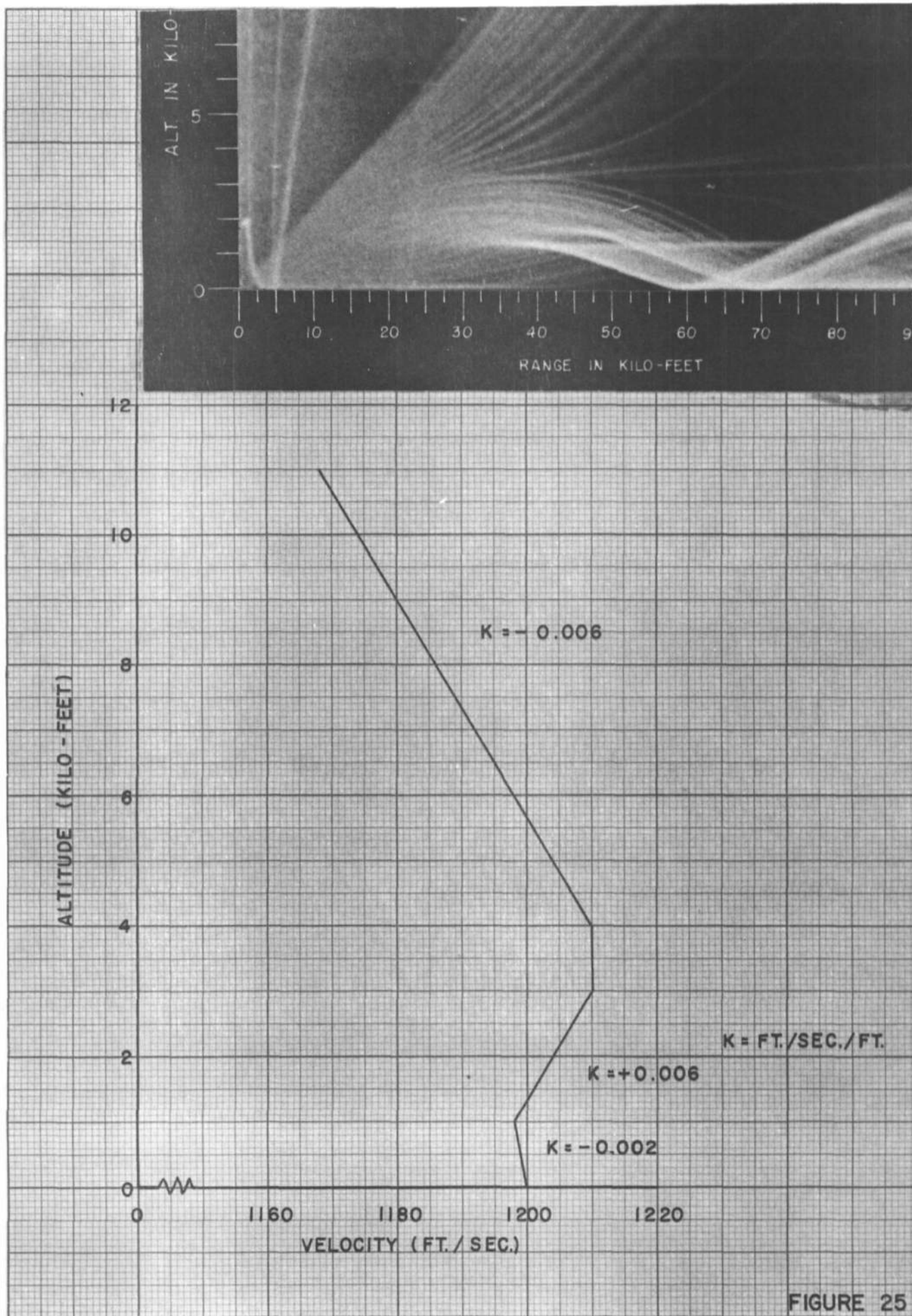
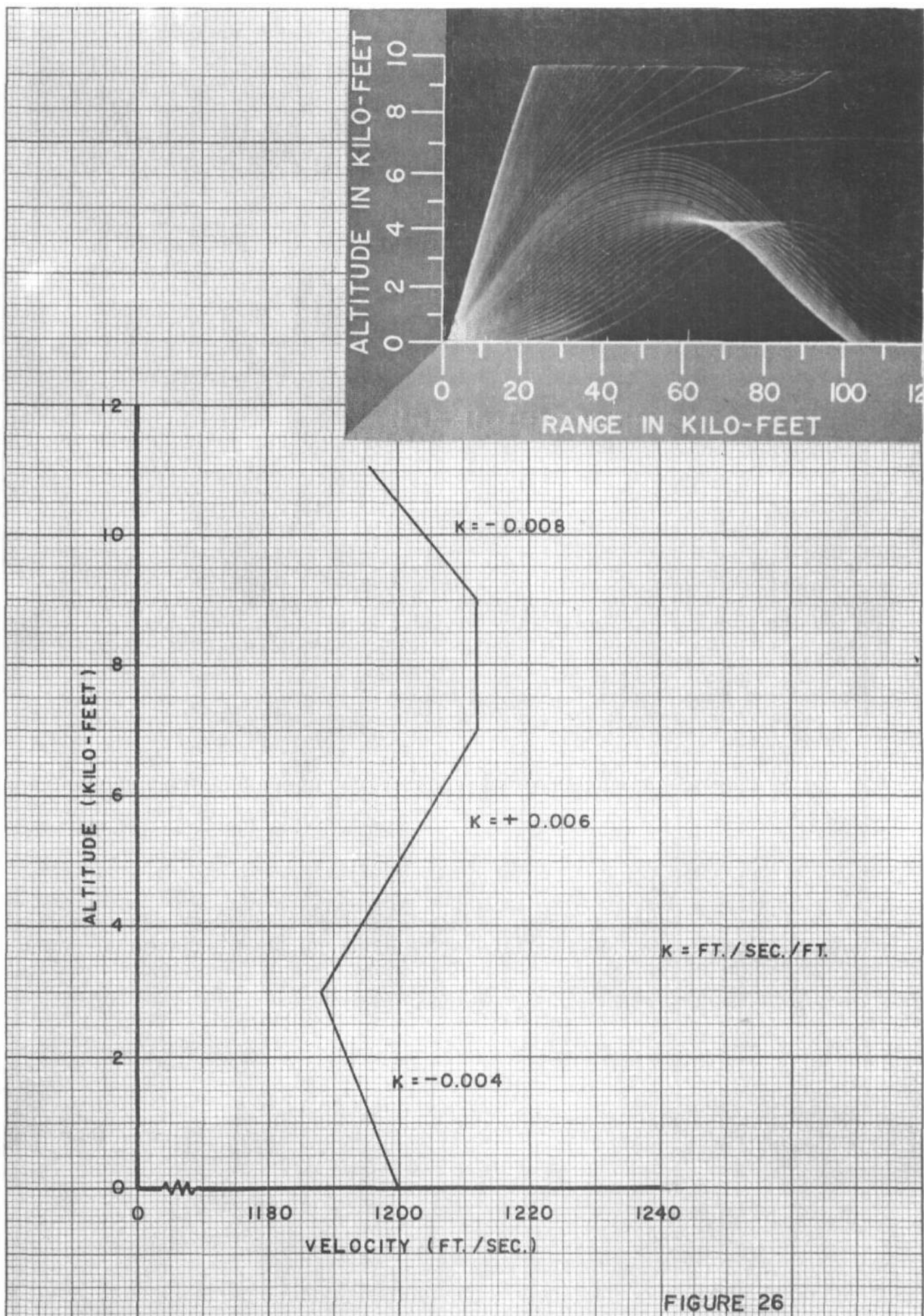


FIGURE 25



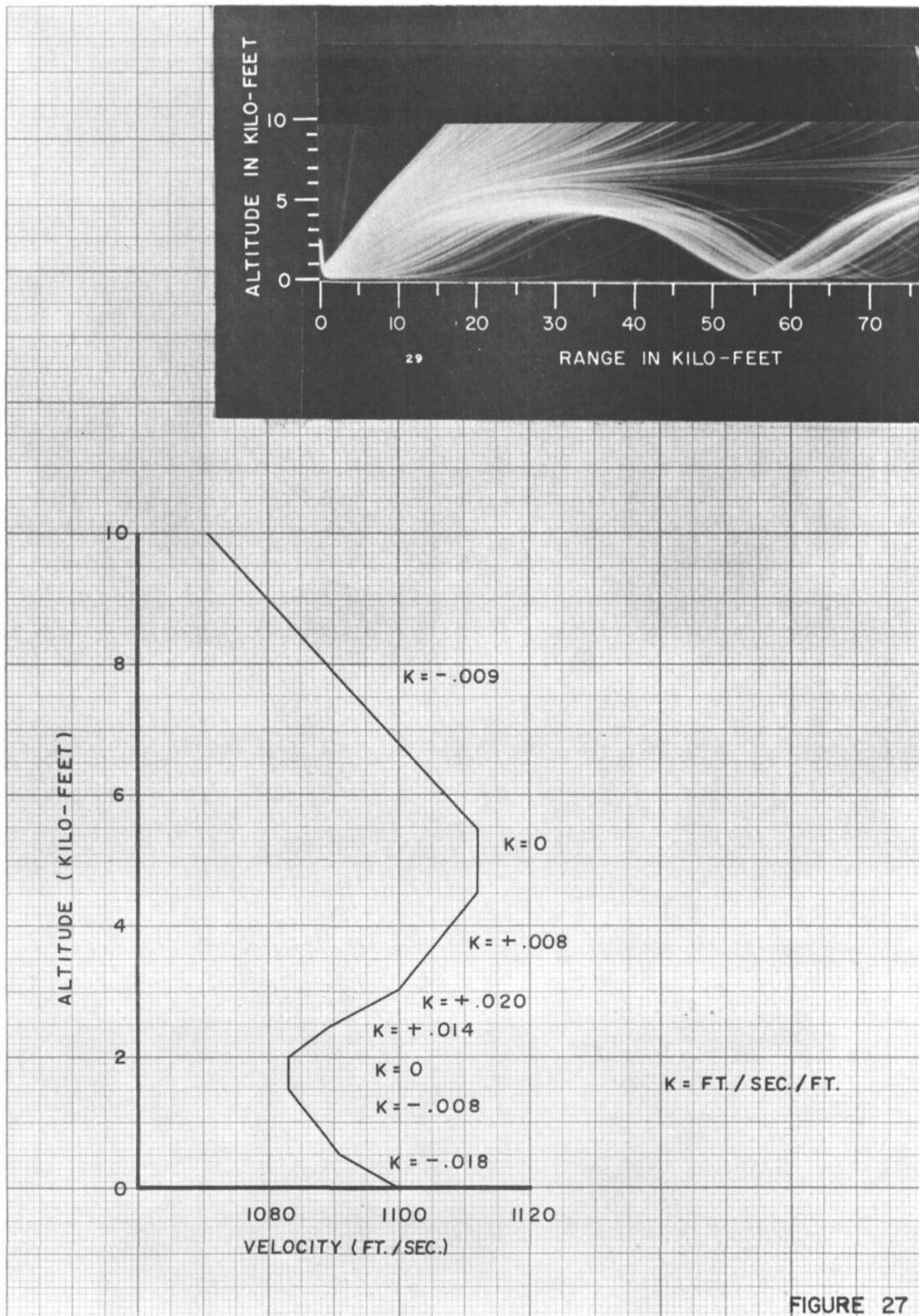


FIGURE 27

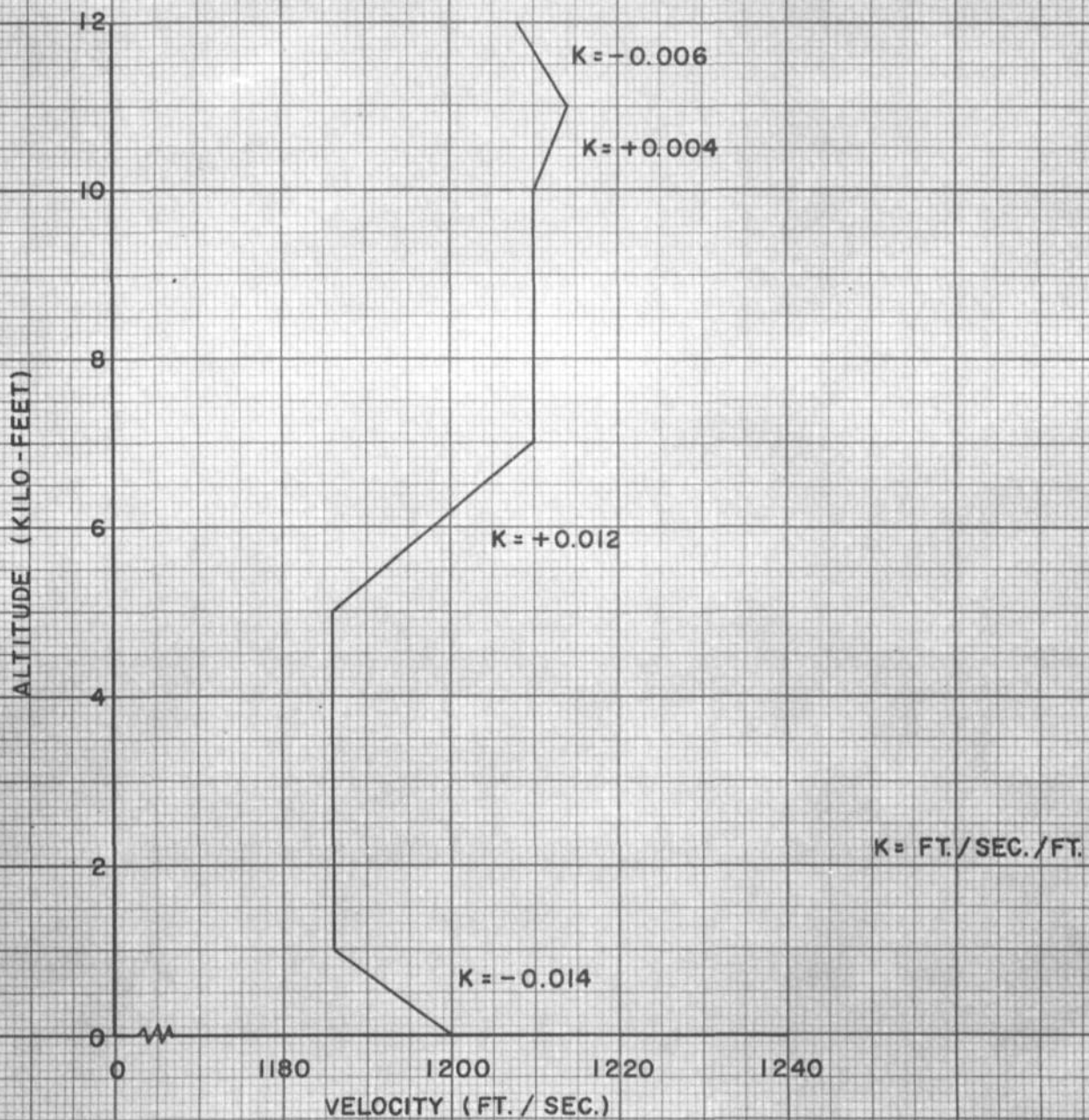
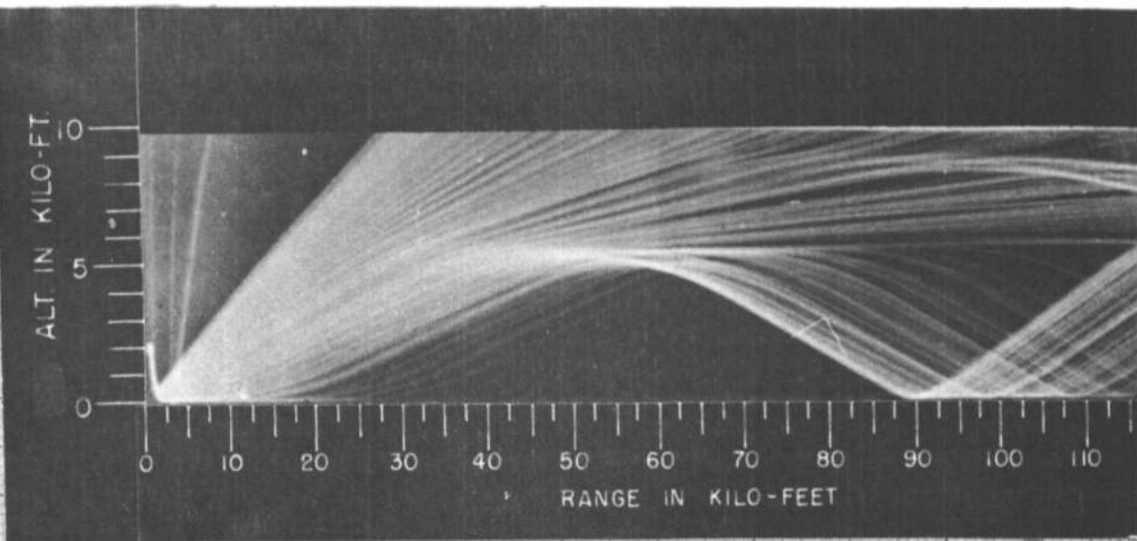


FIGURE 28

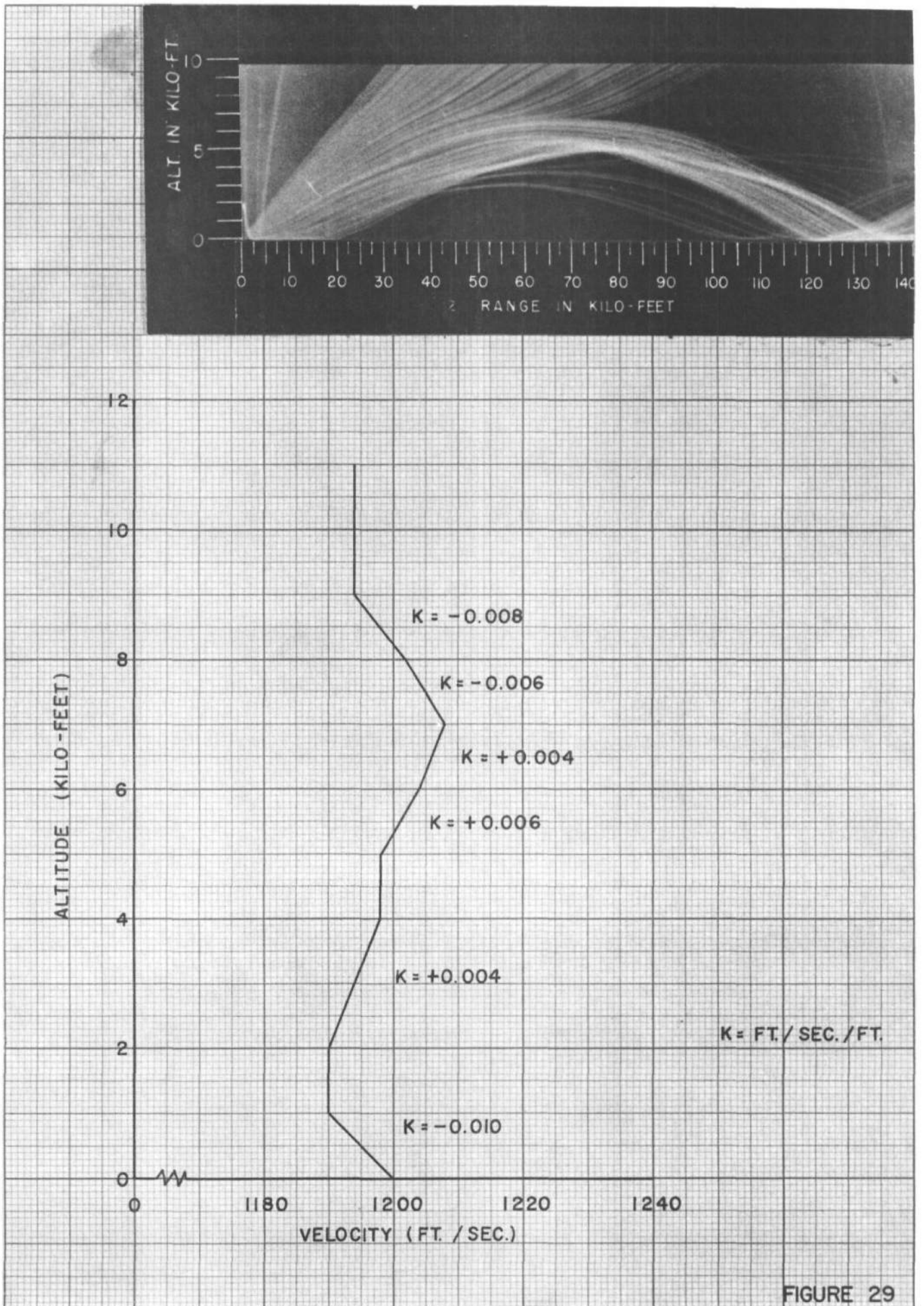


FIGURE 29

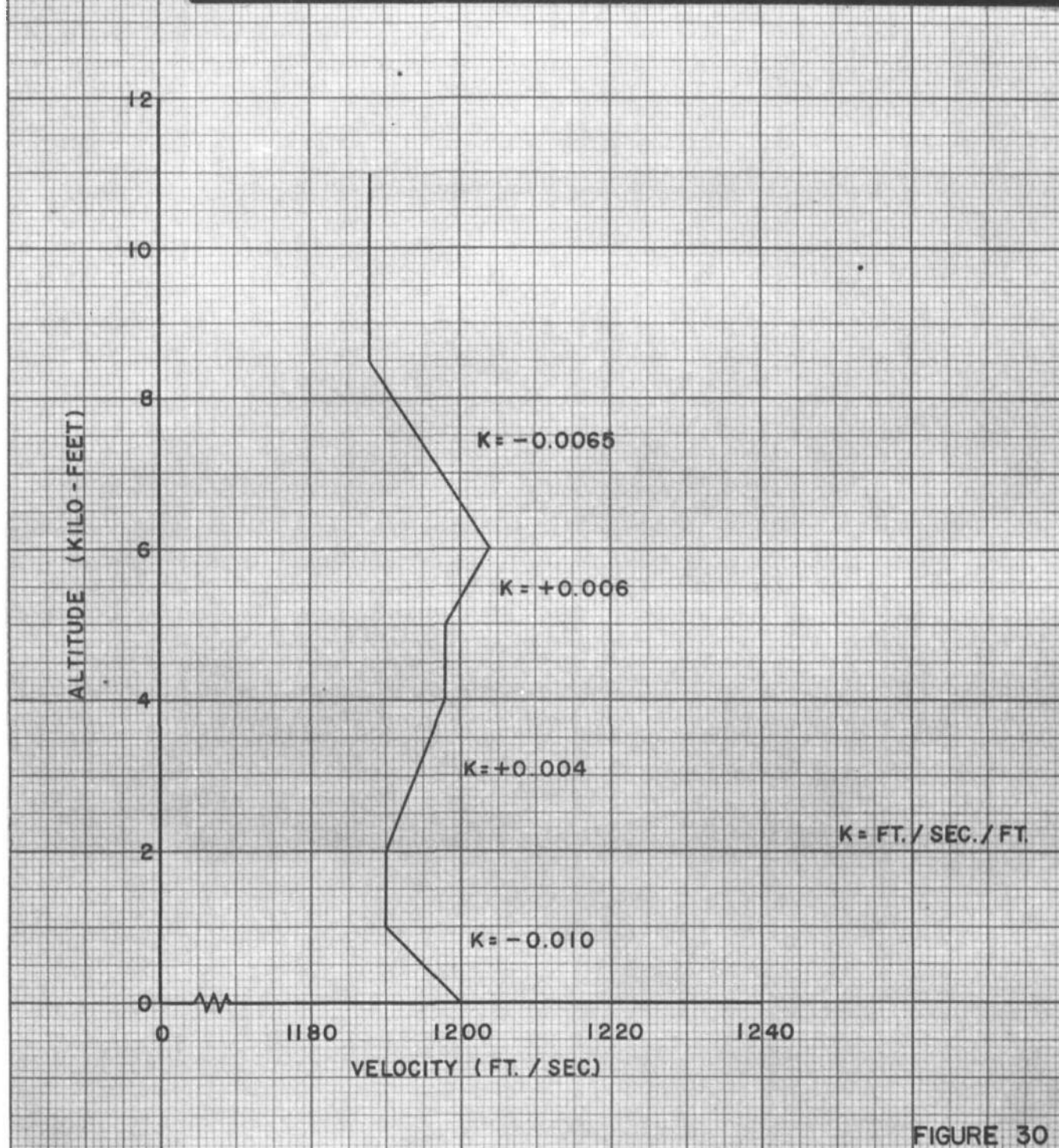
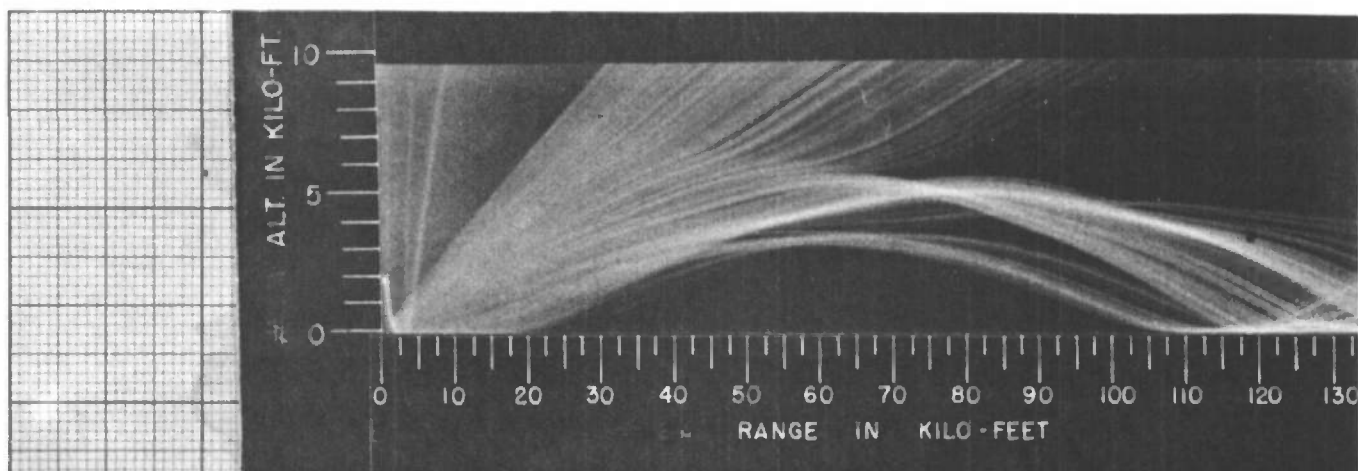


FIGURE 30

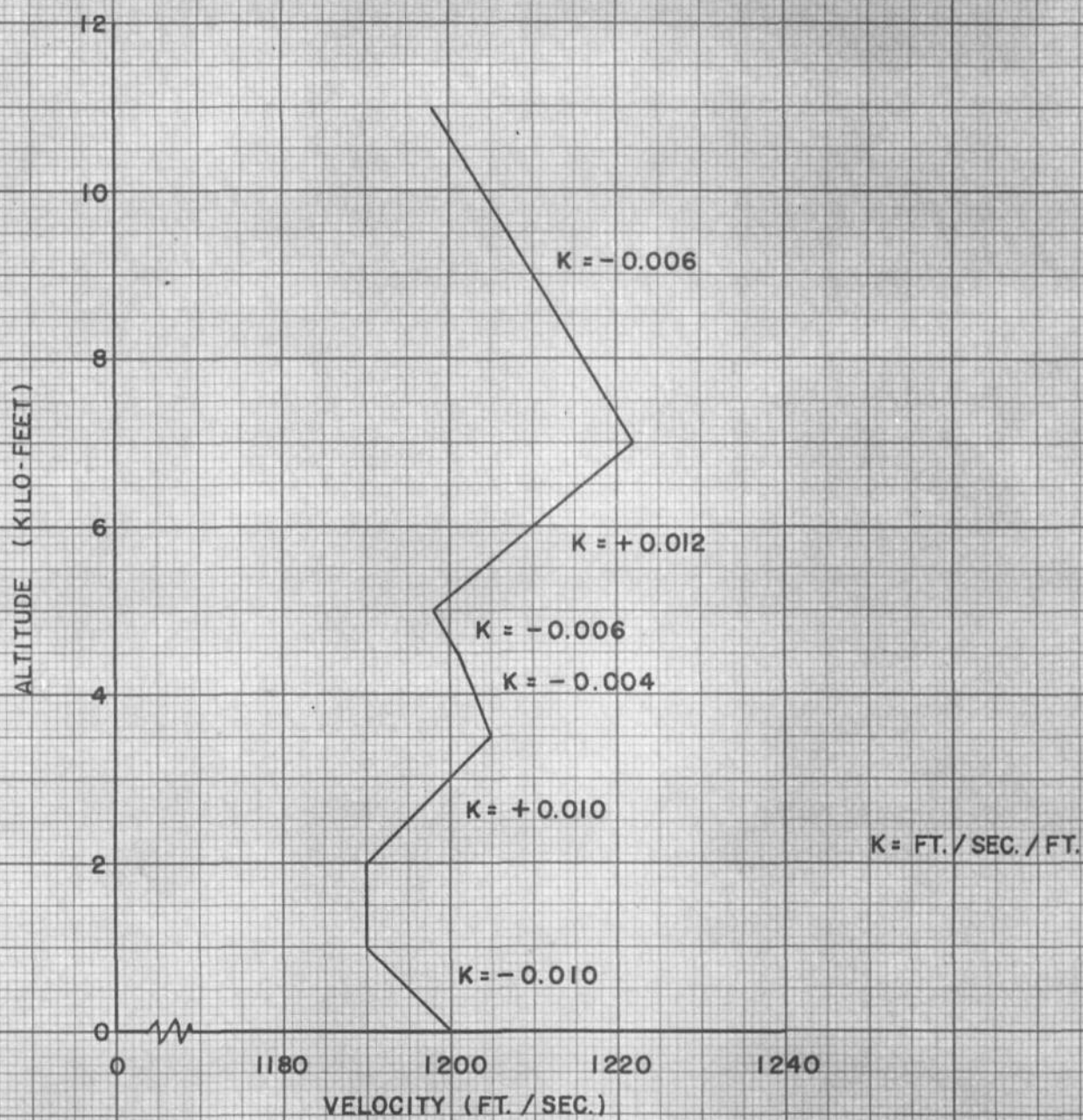
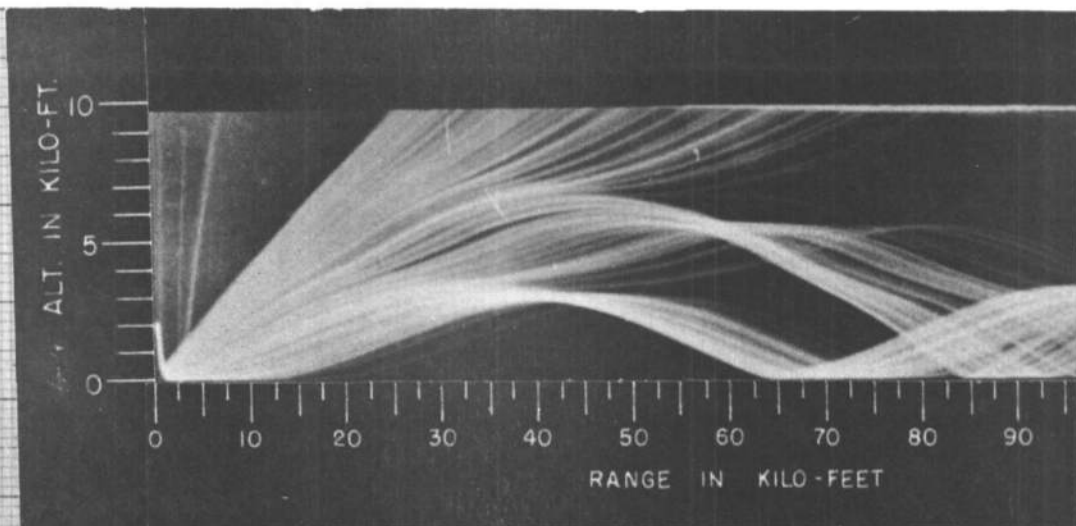


FIGURE 31

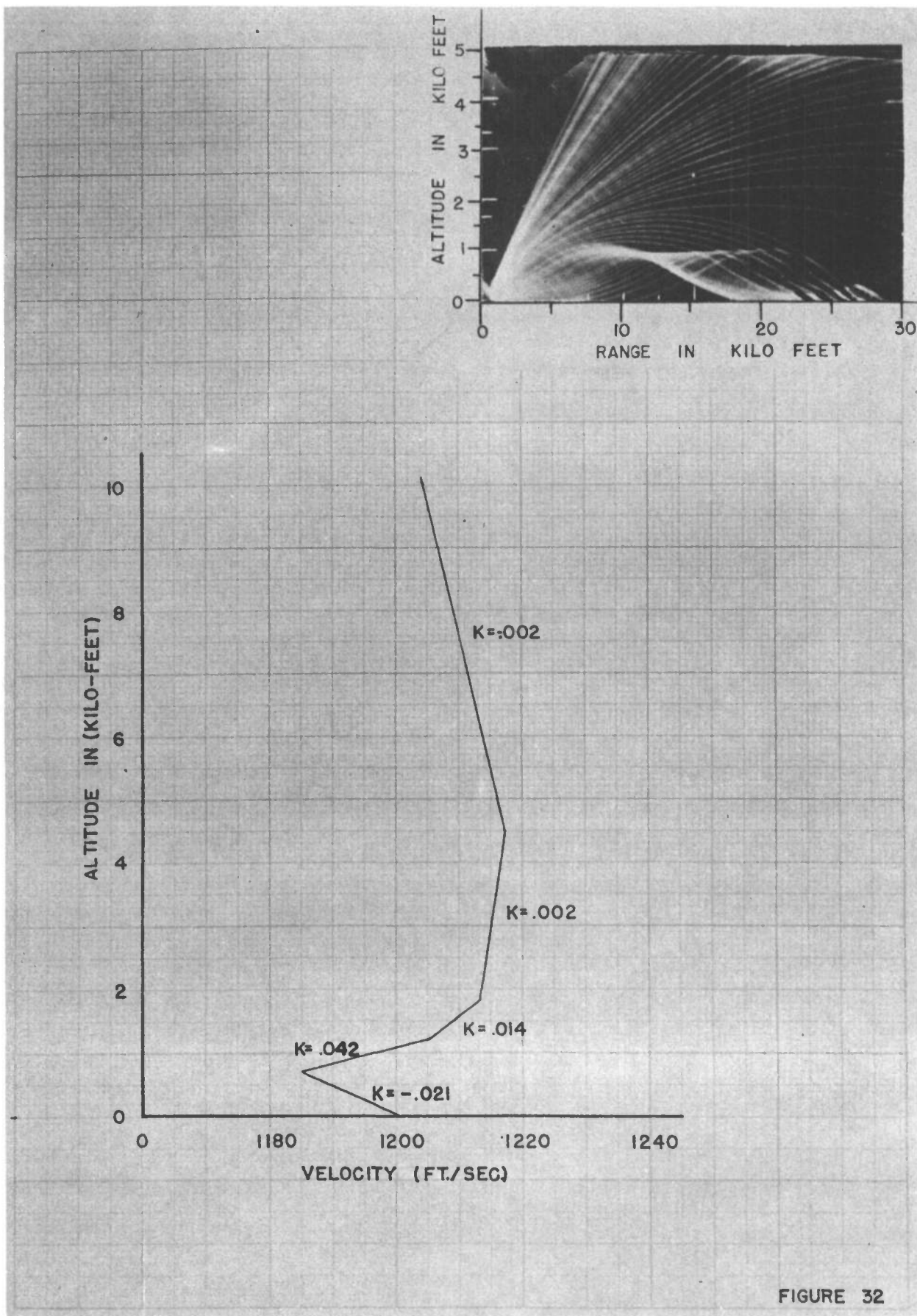


FIGURE 32

DISTRIBUTION LIST

<u>No. of Copies</u>	<u>Organization</u>	<u>No. of Copies</u>	<u>Organization</u>
1	Chief of Ordnance Department of the Army Washington 25, D.C. Attn: ORDTB - Bal Sec	1	Department of National Defence Defence Research Board Suffield Experimental Station Ralston, Alberta, Canada
1	Commanding Officer Diamond Ordnance Fuze Laboratories Washington 25, D.C. Attn: ORDTL - 012	2	Chief, Bureau of Naval Weapons Department of the Navy Washington 25, D.C. Attn: DIS-33
10	Director Armed Services Technical Information Agency Arlington Hall Station Arlington 12, Virginia Attn: TIPCR	2	Commander Naval Ordnance Laboratory White Oak Silver Spring, Maryland Attn: Explosives Division
10	Commander British Army Staff British Defence Staff (W) 3100 Massachusetts Avenue, N.W. Washington 8, D.C. Attn: Reports Officer	1	Chief of Naval Operations Department of the Navy Washington 25, D.C. Attn: Op-36
4	Canadian Army Staff 2450 Massachusetts Avenue Washington 8, D.C.	2	Chief of Naval Research Department of the Navy Washington 25, D.C. Attn: Code 118
	Of Interest To:	2	Director Naval Research Laboratory Anacostia Station Washington 20, D.C.
2	Canadian Armament Research and Development Establishments P.O. Box 1427 Quebec City Quebec, Canada Attn: E.W. Greenwood	1	Officer-in-Charge U.S. Naval Civil Engineering Research and Evaluation Laboratory U.S. Naval Construction Battalion Center Port Hueneme, California
1	Inspection Services Department of National Defence No. 8 Tempo Building Ottawa, Ontario, Canada Attn: L. Barnes	1	Chief, Bureau of Yards and Docks Department of the Navy Washington 25, D.C. Attn: Commander W.J. Christensen

DISTRIBUTION LIST

<u>No. of Copies</u>	<u>Organization</u>	<u>No. of Copies</u>	<u>Organization</u>
1	Commanding Officer and Director U.S. Naval Engineering Experiment Station Annapolis, Maryland	1	Commander Air Force Special Weapons Center Kirtland Air Force Base New Mexico Attn: Research and Development, Mr. Eric Wang
1	Commanding Officer and Director David W. Taylor Model Basin Washington 7, D.C. Attn: Structural Mechanics Division	1	Commander Wright Air Development Division Wright-Patterson Air Force Base Ohio
3	Commander U.S. Naval Ordnance Test Station China Lake, California Attn: Technical Library Editorial Section	1	Director Air University Library Maxwell Air Force Base Alabama
1	Commander U.S. Naval Missile Center Point Mugu, California Attn: Mr. Jerry Overton	4	Commander Air Force Ballistic Missile Division P.O. Box 262 Inglewood 49, California Attn: Dr. George Young
1	Commanding Officer U.S. Naval Weapons Laboratory Dahlgren, Virginia	1	Deputy Chief of Staff, Development Research and Development Directorate U.S. Air Force Washington 25, D.C. Attn: Chief, Research Division
1	Commander Air Research and Development Command Andrews Air Force Base Washington 25, D.C.	1	Deputy Chief of Staff, Operations U.S. Air Force Washington 25, D.C. Attn: Assistant for Atomic Energy, AFOAT
1	Commander Air Proving Ground Center Eglin Air Force Base Florida Attn: PGTRI	1	Director, Project RAND Department of the Air Force 1700 Main Street Santa Monica, California Attn: Dr. Brode
1	Commander Air Force Cambridge Research Center, ARDC L. G. Hanscom Field Bedford, Massachusetts Attn: Geophysical Research Library		

DISTRIBUTION LIST

<u>No. of Copies</u>	<u>Organization</u>	<u>No. of Copies</u>	<u>Organization</u>
3	Commanding General Frankford Arsenal Philadelphia 37, Pennsylvania Attn: Pitman-Dunn Laboratory Library Branch, 0270, Bldg. 40 Mr. H. Sokowlowski	2	Commanding General White Sands Missile Range New Mexico Attn: ORDBS-OM-W, John Day
3	Commanding Officer Picatinny Arsenal Dover, New Jersey Attn: Feltman Research and Engineering Laboratories	2	Chief of Engineers Department of the Army Washington 25, D.C. Attn: Mr. Martin Kirkpatrick Lt. Col. Russell Hutchinson
2	Commanding Officer Rock Island Arsenal Rock Island, Illinois Attn: Dr. A.C. Hanson	2	Commanding General Engineer Research and Development Laboratories U.S. Army Fort Belvoir, Virginia Attn: Dr. T.G. Walsh K.S. Flint, Applied Research Section Mine Warfare and Barrier Branch
1	Commanding Officer Watertown Arsenal Watertown 72, Massachusetts Attn: Laboratory	1	Commanding Officer U.S. Army Chemical Warfare Laboratories Army Chemical Center, Maryland
2	Commanding General Army Ballistic Missile Agency Redstone Arsenal, Alabama Attn: ORDAB-DTR Mr. Wade Dorland C.C. Thornton	1	Director, Operations Research Office Department of the Army 6935 Arlington Road Bethesda, Maryland Washington 14, D.C.
1	Commanding General Army Rocket and Guided Missile Agency Redstone Arsenal, Alabama Attn: Safety Officer, Mr. T.W. Davidson	1	Commanding Officer Office of Ordnance Research Box CM, Duke Station Durham, North Carolina
1	Commanding General U.S. Army Ordnance Missile Command Redstone Arsenal, Alabama Attn: Chief, Occupational Health Service	1	Director, Army Research Office Arlington Hall Station Arlington, Virginia Attn: Geophysics Branch

DISTRIBUTION LIST

<u>No. of Copies</u>	<u>Organization</u>	<u>No. of Copies</u>	<u>Organization</u>
2	President The Ordnance Board Aberdeen Proving Ground Maryland Attn: Captain Decker	1	U.S. Atomic Energy Commission Sandia Corporation P.O. Box 5800 Albuquerque, New Mexico Attn: Physics Division, Mr. W.R. Perret
2	Director Waterways Experiment Station Vicksburg, Mississippi Attn: Mr. G.L. Arbuthnot Mr. William Flathau	1	U.S. Atomic Energy Commission University of California Lawrence Radiation Laboratory P.O. Box 808 Livermore, California Attn: Dr. R.G. Preston
5	Chief, Defense Atomic Support Agency Washington 25, D.C. Attn: Mr. John Lewis	1	Chief, Bureau of Mines Washington 25, D.C.
1	Commanding General Field Command Defense Atomic Support Agency Sandia Base P.O. Box 5100 Albuquerque, New Mexico	1	Armour Research Foundation Illinois Institute of Technology Center Chicago 16, Illinois Attn: Dr. T.H. Schiffman
1	U.S. Atomic Energy Commission Washington 25, D.C. Attn: Technical Reports Library, Mrs. J. O'Leary for Division of Military Application	1	Bolt, Beranek, and Newman, Inc. 50 Moulton Street Cambridge 38, Massachusetts Attn: Francis M. Wiener
1	Executive Secretary Military Liaison Committee to the Atomic Energy Commission 1901 Constitution Avenue, N.W. Washington, D.C.	1	Porter, Urquhart, McCreary and O'Brien O.J. Porter and Company 415-417 Frelinghuysen Avenue Newark, New Jersey Attn: O.J. Porter
2	U.S. Atomic Energy Commission Los Alamos Scientific Laboratory P.O. Box 1663 Los Alamos, New Mexico Attn: Dr. Fred Reines	1	Applied Physics Laboratory The Johns Hopkins University 8621 Georgia Avenue Silver Spring, Maryland
		1	Stanford Research Institute Menlo Park, California Attn: Mr. F. Sauer

DISTRIBUTION LIST

<u>No. of Copies</u>	<u>Organization</u>	<u>No. of Copies</u>	<u>Organization</u>
1	Robert C. Boe Staff Engineer Cook Electric Company Cook Research Laboratories 6401 Oakton Street Morton Grove, Illinois	2	Dr. Leonard Obert Applied Physics Division U.S. Bureau of Mines College Park 1, Maryland
1	Professor W.H. Gardner, Jr. College of Engineering Duke University Durham, North Carolina	1	Mr. R.C. Stange National Board of Fire Underwriters 465 California Street San Francisco 4, California
1	Mr. Norris Haight Ford Motor Company Aeronutronic Division Newport Beach, California	1	Professor J. Neils Thompson Civil Engineering Department University of Texas Austin 12, Texas
1	Mr. Kenneth Kaplan Broadview Research Corporation P.O. Box 1093 Burlingame, California	1	Dr. Robert V. Whitman Massachusetts Institute of Technology Cambridge 39, Massachusetts
1	Dr. Otto LaPorte Engineering Research Institute University of Michigan Ann Arbor, Michigan	1	Professor Walker Bleakney Palmer Physical Laboratory Princeton University Princeton, New Jersey
1	Dr. N.M. Newmark 111 Talbot Laboratory University of Illinois Urbana, Illinois	1	Chief of Staff, U.S. Army Research and Development Washington 25, D.C. Attn: Director/Special Weapons